

# Sensory evolution and ecology of early turtles revealed by digital endocranial reconstructions

Lautenschlager, Stephan; Ferreira, Gabriel; Werneburg, Ingmar

DOI:

[10.3389/fevo.2018.00007](https://doi.org/10.3389/fevo.2018.00007)

*Document Version*

Peer reviewed version

*Citation for published version (Harvard):*

Lautenschlager, S, Ferreira, G & Werneburg, I 2018, 'Sensory evolution and ecology of early turtles revealed by digital endocranial reconstructions', *Frontiers in Ecology and Evolution*. <https://doi.org/10.3389/fevo.2018.00007>

[Link to publication on Research at Birmingham portal](#)

## **Publisher Rights Statement:**

This Document is Protected by copyright and was first published by Frontiers. All rights reserved. It is reproduced with permission

## **General rights**

Unless a licence is specified above, all rights (including copyright and moral rights) in this document are retained by the authors and/or the copyright holders. The express permission of the copyright holder must be obtained for any use of this material other than for purposes permitted by law.

- Users may freely distribute the URL that is used to identify this publication.
- Users may download and/or print one copy of the publication from the University of Birmingham research portal for the purpose of private study or non-commercial research.
- User may use extracts from the document in line with the concept of 'fair dealing' under the Copyright, Designs and Patents Act 1988 (?)
- Users may not further distribute the material nor use it for the purposes of commercial gain.

Where a licence is displayed above, please note the terms and conditions of the licence govern your use of this document.

When citing, please reference the published version.

## **Take down policy**

While the University of Birmingham exercises care and attention in making items available there are rare occasions when an item has been uploaded in error or has been deemed to be commercially or otherwise sensitive.

If you believe that this is the case for this document, please contact [UBIRA@lists.bham.ac.uk](mailto:UBIRA@lists.bham.ac.uk) providing details and we will remove access to the work immediately and investigate.

# Sensory evolution and ecology of early turtles revealed by digital endocranial reconstructions

Stephan Lautenschlager<sup>1</sup>, Gabriel S. Ferreira<sup>2, 3, 4</sup>, Ingmar Werneburg<sup>3, 4, 5\*</sup>

<sup>1</sup>School of Geography, Earth and Environmental Sciences, University of Birmingham, United Kingdom,

<sup>2</sup>Biologia, Faculdade de Filosofia, Ciências e Letras de Ribeirão Preto, Universidade de São Paulo, Brazil,

<sup>3</sup>Seckenberg Center for human evolution and Palaeoenvironment, Germany, <sup>4</sup>Fachbereich

Geowissenschaften, Universität Tübingen, Germany, <sup>5</sup>Leibniz-Institut für Evolutions- und

Biodiversitätsforschung, Museum für Naturkunde, Germany

*Submitted to Journal:*

Frontiers in Ecology and Evolution

*Specialty Section:*

Paleontology

*Article type:*

Original Research Article

*Manuscript ID:*

323974

*Received on:*

24 Oct 2017

*Revised on:*

10 Jan 2018

*Frontiers website link:*

[www.frontiersin.org](http://www.frontiersin.org)

---

### *Conflict of interest statement*

The authors declare that the research was conducted in the absence of any commercial or financial relationships that could be construed as a potential conflict of interest

### *Author contribution statement*

S.L. and I.W. conceived and designed the study, S.L. performed the three-dimensional reconstruction, I.W. provided digital datasets, S.L., G.S.F. and I.W. collected, analyzed and interpreted the data. S.L. and G.S.F. created figures and supplementary data. S.L., G.S.F. and I.W. contributed equally to the discussion, preparation and writing of the paper.

### *Keywords*

Neuroanatomy, sensory adaptation, 3D visualization, Digital endocast, stem-turtle, turtle origin

### *Abstract*

Word count: 184

In the past few years, new fossil finds and novel methodological approaches have prompted intensive discussions about the phylogenetic affinities of turtles and rekindled the debate on their ecological origin, with very distinct scenarios, such as fossoriality and aquatic habitat occupation, proposed for the earliest stem-turtles. While research has focused largely on the origin of the anapsid skull and unique postcranial anatomy, little is known about the endocranial anatomy of turtles. Here, we provide 3D digital reconstructions and comparative descriptions of the brain, nasal cavity, neurovascular structures and endosseous labyrinth of *Proganochelys quenstedti*, one of the earliest stem-turtles, as well as other turtle taxa. Our results demonstrate that *P. quenstedti* had retained a simple tube-like brain morphology with poorly differentiated regions and mediocre hearing and vision, but a well-developed olfactory sense. Endocast shape analysis indicates that an increase in size and regionalization of the brain took place in the course of turtle evolution, achieving an endocast diversity comparable to other amniote groups. Based on the new evidence, we further conclude that *P. quenstedti* was a highly terrestrial, but most likely not a fossorial taxon

### *Funding statement*

This research was funded by FAPESP (Fundação de Amparo à Pesquisa do Estado de São Paulo) grants 2016/03934-2 and 2014/2539-5 to G.S.F. and by SNF (Schweizerischer Nationalfonds zur Förderung der Wissenschaftlichen Forschung advanced postdoc mobility grant P300PA\_164720 to I.W.

### *Ethics statements*

(Authors are required to state the ethical considerations of their study in the manuscript, including for cases where the study was exempt from ethical approval procedures)

*Does the study presented in the manuscript involve human or animal subjects:* No

**Sensory evolution and ecology of early turtles revealed by digital  
endocranial reconstructions**

Stephan Lautenschlager<sup>1,°</sup>, Gabriel S. Ferreira<sup>2,3,4,°</sup> Ingmar Werneburg<sup>3, 4, 5,\*</sup>

<sup>1</sup>School of Geography, Earth and Environmental Sciences, University of Birmingham, Birmingham,  
UK

<sup>2</sup>Biology Department, Faculty of Philosophy, Science, and Letters at Ribeirão Preto, University of  
São Paulo, Ribeirão Preto, Brazil

<sup>3</sup>Senckenberg Center for Human Evolution and Palaeoenvironment (HEP) at Eberhard Karls  
Universität, Tübingen, Germany

<sup>4</sup>Fachbereich Geowissenschaften der Eberhard Karls Universität, Tübingen, Germany

<sup>5</sup>Museum für Naturkunde, Leibniz-Institut für Evolutions- und Biodiversitätsforschung, Berlin,  
Germany

<sup>°</sup> ~~equally~~ contributed equally to the paper

\*Correspondence: Ingmar Werneburg [ingmar.werneburg@senckenberg.de](mailto:ingmar.werneburg@senckenberg.de)

Formatted: Font color: Auto



## Abstract

In the past few years, new fossil finds and novel methodological approaches have prompted intensive discussions about the phylogenetic affinities of turtles and rekindled the debate on their ecological origin, with very distinct scenarios, such as fossoriality and aquatic habitat occupation, proposed for the earliest stem-turtles. While research has focused largely on the origin of the anapsid skull and unique postcranial anatomy, little is known about the endocranial anatomy of turtles. Here, we provide 3D digital reconstructions [and comparative descriptions](#) of the brain, nasal cavity, neurovascular structures and endosseous labyrinth of *Proganochelys quenstedti*, one of the earliest stem-turtles, as well as other turtle taxa. Our results demonstrate that *P. quenstedti* ~~had~~ retained a simple tube-like brain morphology with poorly differentiated regions and mediocre hearing and vision, but a well-developed olfactory sense. Endocast shape analysis indicates that an increase in size and regionalization of the brain took place in the course of turtle evolution, achieving an endocast diversity comparable to other amniote groups. Based on the new evidence [presented herein](#), we further conclude that *P. quenstedti* was a highly terrestrial, but most likely not ~~a~~-fossorial<sub>1</sub> taxon.

**Keywords:** neuroanatomy; sensory adaptation; 3D visualization; digital endocast; stem-turtles; turtle origin

Formatted: Font color: Auto

Formatted: Font color: Auto, English (United States)

## Introduction

Turtles (Testudinata sensu Joyce et al., 2004) are a diverse group of reptiles with an unusual ~~body~~ ~~plan~~: ~~'bauplan'~~ fundamentally different from that of other amniotes. Unique morphological characters, including the anapsid cranial configuration, which lacks temporal fenestrations, and the presence of a bony shell formed by a dorsal carapace and a ventral plastron have long obfuscated the phylogenetic affinities of turtles (Rieppel, 2007; Lyson et al., 2010). While most molecular studies have recovered turtles nested within diapsid reptiles and often as a sister-group to Archosauria (birds and crocodiles) (Hedges and Poling, 1999; Wang et al., 2013; Field et al., 2014), most studies based on comparative anatomy have placed turtles outside of Diapsida (Gauthier et al., 1988; Lee, 1997; Werneburg and Sánchez-Villagra, 2009; Neenan et al., 2013; Scheyer et al., 2017) or alternatively inside Lepidosauromorpha (deBraga and Rieppel, 1997; Rieppel and Reisz, 1999; Li et al., 2008; Liu et al., 2011). The scant fossil record of stem-turtles (i.e., non-Testudines Testudinata) has further obscured the evolutionary origin of this group. Recent discoveries of new species and ~~the~~ reanalysis of existing specimens with novel methodological approaches (e.g. computed tomography and digital visualization) have provided new data to the debate of turtle ancestry (Li et al., 2008; Bever et al., 2015; Schoch and Sues, 2015). These studies found support for the diapsid origin of turtles and produced potential evidence for ~~a~~ closure of the temporal fenestrae early in their evolutionary history (Schoch and Sues, 2015; Lyson et al., 2016; Werneburg, 2015).

Regarding the environmental origin of the group, although all Triassic turtles were clearly terrestrial (Joyce, 2015), data provided by recently described taxa have painted an ambiguous picture regarding the paleoecological setting in which the Testudinata ancestors evolved. While the ~~potentially~~ earliest ~~known~~ ~~potential~~ proto-turtle (i.e., non-Testudinata Pantestudines) *Eumotosaurus africanus* (ca. 260 Ma) has been found in terrestrial environments (Lyson et al., 2016), the somewhat younger *Pappochelys rosinae* (ca. 240 Ma) and *Odontochelys semitestacea* (ca. 220 Ma) were retrieved from lacustrine and deltaic deposits and were considered to have been semi-aquatic (Li et al., 2008; Rieppel, 2013; Schoch and Sues, 2015). In the ~~latter~~ ~~last~~ two taxa, the dorsoventrally flattened, expanded ribs and thickened gastralia have been interpreted as ~~mechanisms to control~~ ~~adaptations for~~ buoyancy ~~control~~ in an aquatic environment (Schoch and Sues, 2015). In contrast, the morphology of the ribs, ~~the as well as the~~ more rigid body wall, powerful forelimbs and ~~a~~ triangular skull, have been considered to represent adaptations to fossoriality in *E. africanus* (Lyson et al., 2016). On the other hand, the type localities of both *P. rosinae* and *O. semitestacea* have also yielded terrestrial taxa (Joyce, 2015; Schoch and Sues, 2017) and, in fact, terrestrial diapsid remains are dominant ~~in at the type locality of~~ the former (Schoch

Formatted: Font color: Auto

and Sues, 2015). Additionally, Joyce (2015) argued in favor of *Odontochelys semitestacea* as a terrestrial proto-turtle, based on its phalangeal formula. Hence, terrestrial, fossorial ~~or~~ and semi-aquatic habits ~~were all previously~~ have all been suggested ~~as the ecological settings during~~ for the early stages of turtle evolution, before the origin of ~~a~~ the protective shell characteristic of the definitely terrestrial stem-turtles (Joyce and Gauthier, 2004; Scheyer and Sander, 2007; Joyce, 2015).

While research on early turtles has focused largely on the acquisition of the anapsid condition and the evolution of the postcranial anatomy employing comparative morphology, histology and genetics, little is known about the endocranial anatomy of stem-turtles (~~as well as~~ or ~~indeed~~ turtles in general). Using micro-computed tomography ( $\mu$ CT) scanning and digital visualization, we here provide a reconstruction of the endocranial anatomy of *Proganochelys quenstedti*, one of the earliest testudines from the Late Triassic of Germany. We further compare the reconstructed brain anatomy with different stem- and crown-turtles (Testudines) and other vertebrate taxa using endocast outline analysis to elucidate related anatomical and ecological aspects of turtle origins.

Formatted: Font color: Auto

## Materials and Methods

For ~~the~~ digital reconstruction of endocranial anatomy (brain, inner ear, neurovascular structures, nasal cavity) two specimens of *Proganochelys quenstedti* from the Late Triassic of Germany were studied: MB 1910.45.2 (Museum für Naturkunde Berlin) from the Baerecke and Limpricht Quarry, Halberstadt (Jaekel, 1918), and SMNS 16980 (Staatliches Museum für Naturkunde Stuttgart) from the *Plateosaurus*-quarry in Trossingen ~~;~~ (Gaffney, 1990). Both specimens consist of nearly complete and articulated cranial skeletons. MB 1910.45.2 shows substantial taphonomic ~~artei~~ arteffacts in the form of anteroposterior shearing and some moderate mediolateral crushing and deformation. However, these ~~artei~~ arteffacts only marginally affect the braincase and the digital reconstruction of the ~~respective~~ various endocranial structures (see Results for more details).

Formatted: Font color: Auto

MB 1910.45.2 was CT scanned at ~~the~~ Leibniz-Institut für Zoo- und Wildtierforschung Berlin / Germany (IZW) using a Toshiba Aquilon ONE medical CT scanner. Scanning parameters ~~properties~~ were set at 225 kV and 300  $\mu$ A resulting in an image stack of 512 x 512 x 213 pixels and a voxel size of 2.0 mm per slice. The dataset was subsequently 'upsampled' (1024 x 1024 x 426 pixels, 0.5 mm effective voxel size) by averaging the existing slice data. This process does not increase the actual resolution of the data, but provides more slices available for segmentation permitting clearer identification of features and resulting in smoother surface models.

Formatted: Font color: Auto

SMNS 16980 was scanned at [the Riedberg Campus of Goethe-Universität Frankfurt](#) / Germany using a Phoenix Nanotom m scanner. Due to [the its](#) relatively large size, the specimen was scanned in three stages. The resulting image stacks were combined into a single stack with 3583 x 4011 x 5658 pixels and a voxel size of 0.025 mm per slice. The dataset was subsequently downsampled (870 x 954 x 1161 pixels, 0.1 mm voxel size) to permit further processing and segmentation.

Formatted: Font color: Auto

Datasets [of for](#) both specimens were imported into Avizo 8 (Visualisation Science Group) for the segmentation of endocranial structures. Due to [the poor greyscale-grayscale](#) attenuation (in particular for SMNS 16980), [the segmentation process](#) was performed manually using the paintbrush and interpolation tools in the Avizo segmentation editor [\(both reconstructions performed by the first author for consistency following Balanoff et al. 2016\)](#). 3D surface models and volumes were created to visualize the endocranial components. In addition, surface models of the individual structures were downsampled to a degree that allowed for small file sizes but preserved all details, and were exported as separate OBJ-files for the creation of the interactive 3D-figures provided in the supplementary material as outlined in Lautenschlager (2014b) using Adobe 3D reviewer (Adobe Systems Inc.).

Formatted: Font color: Auto

Formatted: Font color: Auto

To provide a basis for comparisons, the endocranial anatomy of nine extant turtles and of one additional stem-turtle, *Naomichelys speciosa* (FMNH PR273), was reconstructed in the [same](#) manner [as](#)-described above. FMNH PR273 was scanned at [the Institut für Naturwissenschaftliche Archäologie at the Universität Tübingen](#) at a resolution of 0.1 mm resulting in an image stack [with of 1068 x 1382 x 622 pixels](#). The [following](#) extant species were scanned at the Steinmann-Institut für Geologie, Mineralogie & Paläontologie / Rheinische Friedrich-Wilhelms-Universität Bonn / Germany and at [the Museum für Naturkunde Berlin](#) / Germany: *Podocnemis unifilis* (SMF 55470), *Chelodina reimanni* (ZMB Herpetologie 49659), *Emydura subglobosa* (PIMUZ lab# 2009.37), *Pelodiscus sinensis* (IW576-2), *Chelonia mydas* (ZMB 37416 MS), *Macrochelys temminckii* (TCGT, Teaching collection Geowissenschaften Towisse), *Emys orbicularis* (WGJ 1987a), *Platysternon megacephalum* (SMF 69684), *Malacochersus tornieri* (SMF 58702) (see Supplemental [Information-Material](#) for [collection-Collection](#) abbreviations). Data derived from the reconstructions was further used for a shape analysis of [the](#)-brain morphology.

Formatted: Font color: Auto

Formatted: Font color: Auto

Formatted: Font color: Auto

Due to the absence of unambiguous and [clearly-consistently](#) identifiable landmarks on the endocast across different amniote taxa, outline shape analysis was performed to quantify morphological differences. Although this approach uses only two-dimensional outlines (in contrast to three-dimensional landmarks), it allows [for the](#) quantification of shape data [of for](#) geometries lacking homologous landmarks (Haines & Crampton, 2000). For shape analysis, [a](#) sagittal cross-

sections through the surface models of ~~each the~~ brain (i.e., ~~digital~~ cast of the endocranial cavity) ~~were-was~~ produced in Avizo for ~~all-each~~ reconstructions. Contours of the two-dimensional cross-sections were imported into tpsDig2.16 (Rohlf, 2010), ~~digitised-digitized~~ and saved as 1000 x/y-coordinate pairs. All outline data were subsequently analyzed in PAST ~~23, 17~~ (Hammer et al., 2001) ~~to-perform~~ using Fast Fourier transformation (FFT) and principal components analysis (PCA) ~~usingwith, the hangle module~~ as outlined in Crampton & Haines (1996) and Lautenschlager (2014a). Outlines were smoothed ten times to eliminate pixel noise, and ~~24-23~~ Fourier harmonics were found to describe the outlines of all sampled taxa ~~sufficiently (average Fourier power > 99%) (see also~~ ~~sSupplementary Material)~~. In addition to the reconstructed endocasts, further outlines of 52 taxa were collected from the literature (Hopson, 1979; Franzosa, 2004; Neenan and Scheyer, 2012; Bona and Paulina-Carabajal, 2013; Carabajal et al., 2013; George and Holliday, 2013; Herrera et al., 2013; Holloway et al., 2013; Laab et al., 2017; Paulina-Carabajal et al., 2017; von Baczko and Desojo, 2016; Lautenschlager and Butler, 2016; Jirak and Janacek, 2017; Pierce et al., 2017; and Digimorph) for different turtle, archosauromorph, lepidosauromorph and other amniote taxa (for list of taxa see Table S2). ~~These outlines were redrawn in Adobe Illustrator to ensure sufficient resolution for the digitization process.~~ For PCA, ~~all-taxa-wereeach~~ taxon was assigned to a phylogenetic and an ecological (marine, freshwater, terrestrial, fossorial) group. To test for significant differences between those groups, we also conducted a non-parametric MANOVA test (Anderson, 2001) using PC scores representing 95% of total variance ~~transformed into an Euclidean distance matrix, and replicated with~~ 10000 permutations ~~and compared using Bonferroni correction for the post-hoc analysesfor test significance of pairwise distances.~~

Formatted: Font color: Auto

Formatted: Font color: Auto

Formatted: Font color: Auto

Formatted: Font color: Auto

Formatted: Font color: Auto

Formatted: Font color: Auto

Formatted: Font color: Auto

Formatted: Font color: Auto

Formatted: Font color: Auto

## Results

### Endocranial anatomy

Formatted: Font color: Auto

Formatted: Font: Italic, Font color: Auto

The reconstruction of MB 1910.45.2 (Figures 1A–1D) provided most details of the endocranial anatomy, but exhibited some moderate medio-lateral deformation. In comparison, the reconstruction of SMNS 16980 (Figures 1E–1H) showed no obvious artifacts, but the poor ~~greyscale-grayscale~~ contrast permitted only a few structures (i.e., brain, pituitary fossa and some cranial nerves) to be visualized. In combination, both specimens allowed for a detailed reconstruction of most endocranial components.

The brain endocast is anteroposteriorly elongate and straight in both specimens, with only moderate cephalic and pontine flexures (Figures 1B, 1F). The endocasts are tubular and mediolaterally narrow without prominent expansion or constriction of the fore-, mid- or hindbrain

175 regions. The close similarity of these features in both specimens confirms that this morphology is  
176 natural and unlikely to be a result of taphonomic deformation. The olfactory nerve (CN I)  
177 contributes approximately a third to half of the full endocast's length, but a clear distinction  
178 between the base of the olfactory nerve and the cerebral hemispheres is not visible. The olfactory  
179 bulbs are only weakly reproduced by the ventral surfaces of the nasals. Cerebral hemispheres or  
180 distinct optic lobes are not visible in ~~both-either~~ specimens, suggesting that ~~either-both~~ structures  
181 ~~was-were~~ very small and/or that the venous sinus and the dura mater obscured the underlying  
182 morphology.

183 The midbrain region is confluent with the forebrain and only weakly demarcated. The only  
184 distinguishing feature is a dorsal expansion extending above the level of the olfactory nerve. This  
185 dural peak or cartilaginous rider (Zangerl, 1960; Gaffney and Zangerl, 1968; Paulina-Carabajal et  
186 al., 2017) is more prominently developed in MB 1910.45.2 (Figure 1B). In SMNS 16980, the dorsal  
187 expansion is shallower and somewhat separated from the main body of the midbrain by a bony  
188 margin, suggesting that this structure corresponds to the cartilaginous portion of the supraoccipital,  
189 which ends abruptly anteriorly in *Proganochelys quenstedti* (Gaffney, 1990). The pituitary fossa is  
190 visible in SMNS 16980 and forms a pendant pocket, projecting ventrally from the main body of the  
191 midbrain endocast.

192 The hindbrain region is anteroposteriorly short and not constricted mediolaterally between  
193 the endosseous labyrinths. Floccular lobes are not visible. Posteriorly, the hindbrain exits the  
194 braincase through the foramen magnum, which is oval and wider than high in SMNS 16980 and  
195 slightly higher than wide in MB 1910.45.2. The latter may be the result of the mediolateral  
196 compression of this specimen.

197 The nasal cavity is very enlarged when compared to the other sampled taxa (Figures 2, 3;  
198 Table 1). The strong lateral compression of ~~MB 1910.45.2 the latter specimen~~ may be responsible  
199 for the seemingly increased volume, and, hence, we consider the reconstruction of the nasal cavity  
200 in SMNS 16980 more reliable. Usually, three portions of the nasal cavity can be identified in turtles  
201 and other reptilians (Parsons, 1959, 1970; Halpern, 1992; Paulina-Carabajal et al., 2017): the  
202 vestibulum nasi, which connects the nasal chamber to the external nares; the ductus  
203 nasopharyngeus, connecting the nasal chamber to the choanae; and the cavum nasi proprium, the  
204 chamber itself, bounded anteriorly by the vestibulum, posteroventrally by the ductus, and  
205 posterodorsally by the olfactory nerve (CN I). The ductus nasopharyngeus can be distinguished  
206 from the rest of the nasal cavity in *P. quenstedti* as two ventrolateral projections (Figure 1). A  
207 proper duct ~~was not expected~~ (at least not bounded by bone) ~~was not expected~~, since the choanae in  
208 *P. quenstedti* are very extensive, and occupy almost the whole ventral surface of the nasal cavity.

Formatted: Font color: Auto

The vestibulum on the other hand is short, as in most other turtles (Paulina-Carabajal et al., 2017), connected to the large cavum nasi proprium, which constitutes most of the nasal cavity. The cavity as a whole is considerably broad and also high in comparison (Figures 2, 3) to several other taxa (Carabajal et al., 2013; Paulina-Carabajal et al., 2017).

Formatted: Font color: Auto

The endosseous labyrinth is reconstructed only for MB 1910.45.2-only, as the grey-scale attenuation did not allow a-differentiation of the respective-bony housing in SMNS 16980. It is dorsoventrally compressed and compact. The anterior and posterior semicircular canals are small, and anteroposteriorly longer than high and have low internal radii. The crus communis is also very low in comparison to other taxa (Carabajal et al., 2013; Mautner et al., 2017; Paulina-Carabajal et al., 2017; Ferreira et al., in press) and-which results in an almost horizontal orientation of the anterior and posterior semicircular canals (Figure 4). The lateral semicircular canal barely extends mediolaterally from the vestibulum. The cochlear duct is expanded ventrally, but short. The canal of the fenestra ovalis is clearly visible projecting anterolaterally from the vestibulum.

Formatted: Font color: Auto

The proximal portion of the majority of cranial nerves could be reconstructed for MB 1910.45.2 (Figure 1), whereas only some of the larger nerve canals are visible in SMNS 16980. The optic nerves (CN II) exit the braincase through two large (3 mm in diameter each) foramina anteriorly and ventrally from the cerebral region of the endocast in MB 1910.45.2. Posterior and lateral to CN II, the oculomotor (CN III) and possibly the trochlear nerve (CN IV) (Gaffney, 1990) originate ventrolaterally. In SMNS 16980, CN II-IV could not be reconstructed. The foramina through which those three cranial nerves (II-IV) exit the braincase are formed by the laterosphenoid (=“pleurosphenoid”) (Gaffney, 1990; Bhullar & Bever, 2009). This is the second *P. quenstedti* specimen with a preserved laterosphenoid, however the fact that this ossification is severely crushing-crushed refrain-leads us to refrain from further-commenting further on the-its morphology of this ossification. The trigeminal nerve (CN V) is large (ca. 6 mm in diameter) and exits the braincase laterally in both specimens through the prootic foramen. Based on both specimens (as well as other specimens described by Gaffney, 1990) we confirm that this foramen is surrounded exclusively by the prootic bone, contrary to Bhullar & Bever’s (2009) interpretation that the laterosphenoid would form its anterior margin. A separation of the ophthalmic branch (CN V<sub>1</sub>) is apparent on the right side in MB 1910.45.2, but this could be the-a result of the high degree of distortion of this specimen.

The abducens nerve (CN VI), clearly visible in both specimens, originates from the ventral surface of the endocast. It pierces the basisphenoid through the foramen nervi abducens and enters laterally the pituitary fossa laterally, which is bottomed by the sella turcica (Gaffney, 1990). Posterior to CN V, the facial nerve (CN VII) exits the braincase laterally through the prootic. In MB

1910.45.2, a distal branching of CN VII outside the braincase wall is visible, also on the prootic bone. The vestibulocochlear nerves (CN VIII) could not be reconstructed in either specimen. The foramina for the CN VIII branches are usually very small and may lie on cartilaginous structures (Gaffney, 1979), so they are not expected to leave unambiguous traces on fossilized skulls. The glossopharyngeal (CN IX), vagus (CN X) and accessory nerves (CN XI) originate immediately posterior to the endosseous labyrinth and exit the braincase through the anterior jugular foramen in MB 1910.45.2. Although the sutures are not very clear, this foramen is thought to be formed by the exoccipital, basioccipital and opisthotic in *P. quenstedti* (Gaffney, 1990). In SMNS 16980, a large nerve canal originates ~~from in~~ a more dorsolateral position (Figure 1). Due to the low resolution, it is unclear whether this canal represents the anterior jugular foramen or ~~more likely~~ parts of the longitudinal sinus, though the latter is more likely. The hypoglossal nerve (CN XII) is transmitted through a single foramen on each side of the basioccipital (posterior to the jugular foramen) in both specimens.

#### *Endocast outline analysis*

The morphology of the endocast of *P-Proganochelys quenstedti* was compared to different turtles and other amniote taxa using shape analysis. The PCA results show that the first three PCs account for 71.7% (Table 2) of the brain endocast outline shape variation (Figures 5, 6). In ~~all no~~ PC plots ~~is~~ there ~~is no~~ clear separation between either the phylogenetic or the ecological groups considered. However, the PERMANOVA tests support ~~s significant differences of that~~ Lepidosauromorpha differs significantly from Archosauromorpha ( $p = 0.0006$ ) and from Testudinata ( $p = 0.003$ ) ~~and~~ ~~nealthough these tests find no~~ significant differences between the ecological groups (Table 3). The outgroup *Diadectes* is recovered consistently in a position inside the morphospace occupied by ~~the~~ other groups, whereas *P. quenstedti* ~~is displaced from the occupied area in all plots; however, on the~~ PC1 axis, *Kawingasaurus* is even more displaced ~~on in~~ the positive direction (Figures 5, 6). *P. quenstedti* is distant from other turtles and the minimum spanning-tree (see Supplementary Material) ~~shows a places it~~ closer ~~position~~ to the lepidosauromorphs *Placodus* and *Chalarodon*, and to the archosauromorph *Pseudopalatus*, on the PC1/PC2, PC1/PC3 and PC2/PC3 plots, respectively. ~~Considering~~ With regard to the ecological morphospaces, *P. quenstedti* is similarly found in a position outside ~~of~~ all the groups, except on the PC1/PC3 plot, ~~in on~~ which it is inside the fossorial morphospace and much very close to the terrestrial occupied morphospaces one (Figure 5D).

#### Discussion

Formatted: Font: Italic, Font color: Auto

Formatted: Indent: First line: 0"

Formatted: Font color: Auto

Formatted: Font color: Auto



277

278 **Ancestral condition for Testudinata**

279 Even though more taxa have been assigned to the turtle stem-lineage recently (Li et al., 2008;  
 280 Lyson et al., 2010; Schoch and Sues, 2015), *Proganochelys quenstedti* remains one of the most  
 281 important stem-turtles, given its phylogenetic position as the earliest shelled turtle with a  
 282 completely preserved skull (Parsons, 1959, 1970; Halpern, 1992; Joyce et al., 2016). Its endocast is  
 283 a relatively simple structure when compared to that of crown-turtles (Carabajal et al., 2013;  
 284 Mautner et al., 2017; Paulina-Carabajal et al., 2017; Ferreira et al., in press). It has a tube-like  
 285 shape, with only small pontine and cephalic flexures and poorly differentiated brain regions. As in  
 286 other amniotes, the portion between the fore- and midbrain is the most voluminous, but this is  
 287 achieved exclusively by an increase in height, since ~~the endocast its width~~ is nearly constant in  
 288 width as long as the over its entire endocast length (Figure 1). Another striking feature is the pendant  
 289 pituitary fossa, which is very common in archosaurs (Witmer et al., 2008; Lautenschlager and  
 290 Butler, 2016; Araújo et al., 2017; Pierce et al., 2017), but does not occur in extant turtles, in which  
 291 the dorsum sellae and the sella turcica are aligned, positioning the pituitary fossa approximately at  
 292 the same level as the posterior portions of the endocast (Figures 2, 3). Although the pituitary fossa  
 293 of turtles can also house other smaller structures (e.g., internal carotid and abducens nerve) the size  
 294 of the pituitary gland should be at least partially responsible for ~~a the~~ larger size of the fossa in *P.*  
 295 *quenstedti*. A similar condition was found for sauropod and theropod dinosaurs (Witmer et al.,  
 296 2008), in which enlarged pituitary glands have been linked to larger body sizes (Edinger, 1942).  
 297 While *P. quenstedti* reached a carapace length size of at least 67 cm ~~of carapace length~~ (based on  
 298 MB 1910.45.2) (Gaffney, 1990), it was not one of the largest turtles, being much smaller than some  
 299 extant turtles (e.g., up to 150-200 cm in *Chelonia mydas* and *Pelochelys cantorii*) (Angielczyk et  
 300 al., 2015) and meiolanids (Gaffney, 1996). Turtles included in our sample ~~with that are~~ comparable  
 301 in size to *P. quenstedti*, such as *Podocnemis unifilis* and *Macrochelys temminckii* (up to 68 and 66  
 302 cm of carapace length) (Angielczyk et al., 2015), and also *Chelonia mydas*, do not show a pendant  
 303 pituitary fossa (Figures 2, 3). An alternative explanation is that it is not the pituitary fossa that is  
 304 larger in *P. quenstedti*, but rather the brain that was comparatively smaller. Indeed, in our sample,  
 305 this taxon has the lowest value for the ratio endocast volume/basicranial length (Table 1),  
 306 supporting the hypothesis that the brain increased in size during turtle evolution.

307 The brain endocast in turtles does not seem to be consistent with general skull anatomy.  
 308 Taxa with higher/lower and wider/thinner endocasts do not possess similar skull proportions,  
 309 which, ~~on the contrary,~~ seems more related to the size and shape of the adductor chamber and the  
 310 associated supraoccipital and squamosal crests (Figure 7). Proportional changes observed in the

adductor chamber throughout the turtle lineage rather reflect the distinct volume and size of the external jaw adductor musculature in different taxa (Claude et al., 2004; Foth and Joyce, 2016; Foth et al., 2017; Ferreira and Werneburg, in press). Also, the position of the exits of the cranial nerves ~~change~~ only slightly ~~change~~, even with profound changes in the arrangement of related structures such as ~~the eyes position~~ and ~~muscles anatomy~~. For example, in *P. quenstedti* the external jaw adductor musculature innervated by the trigeminal nerve (CN V<sub>3</sub>) is vertically oriented and entirely positioned anteriorly to the quadrate (Ferreira and Werneburg, in press), while in crown-turtles it extends far posteriorly, following the enlargement of the supraoccipital and squamosal crests (Poglayen-Neuwall, 1953; Werneburg, 2011, 2013). However, the relative position of the exit of CN V remains roughly the same through turtle evolution when compared to the remainder of the endocast and the surrounding bones (Figure 7). Hence, the actual change that occurs when the muscles expand posteriorly involves only ~~a~~ growth and reorientation of distal V<sub>3</sub>-branches and not a repositioning of the trigeminal nerve foramen (Poglayen-Neuwall, 1953; Schumacher, 1973).

### Sensory capabilities of *Proganochelys*

The endosseous labyrinth of *Proganochelys quenstedti* is slightly distinct from that of crown-turtles in being more compact and robust, with short and thick semicircular canals and a low crus communis resulting in almost horizontally oriented canals (Figure 4). The anterior and posterior semicircular canals (ASC and PSC, respectively) are nearly at the same level as the lateral semicircular canal (LSC), whereas in other turtles the ~~former-first~~ two run dorsally in relation to the ~~latter-last~~ (Carabajal et al., 2013; Mautner et al., 2017; Paulina-Carabajal et al., 2017; Ferreira et al., in press). The angle between ~~the~~ ASC and LSC is also very wide (Table 1), with similar values to meiolaniids and tortoises (Paulina-Carabajal et al., 2017). This combination of features suggests that the semicircular canals of *P. quenstedti* were not very sensitive during movements ~~along-within~~ the sagittal (head moving up and down) and coronal planes (head tilt) (Brichta et al., 1988; Spoor et al., 2007; David et al., 2010). Instead, the LSC was likely more effective in stabilizing gaze during yaw movements (head moving left and right). Thus, the labyrinth anatomy of *P. quenstedti* indicates ~~it-as~~ ~~this species was~~ slow and non-agile (Spoor et al., 2007; David et al., 2010), compatible with a highly terrestrial and possibly fossorial lifestyle. This is also tentatively indicated by ~~the-its position in~~ morphospace ~~occupations~~ outside of, but close to, a terrestrial and fossorial ~~habitat-groupings~~ in the shape analysis (Figure 6).

Although *P. quenstedti* cervical vertebrae were capable of ~~a~~ certain ~~level of~~ mobility (Werneburg et al., 2015a), its short neck coupled with ~~the~~ relatively low carapace, strong osteoderms on the dorsal neck surface and cervical ribs (Gaffney, 1990) imply restricted mobility

345 along the same planes (sagittal and coronal) (Werneburg et al., 2015a, 2015b) as indicated by its  
346 labyrinth morphology. Crown-turtles, however, evolved longer necks and several taxa are capable  
347 of complex and, sometimes, very fast neck and head movements (Poglayen-Neuwall, 1953; Herrel  
348 et al., 2008; Werneburg et al., 2015a, 2015b). This could be related to the apparent increase in size  
349 of the semicircular canals in crown-turtles (Spoor, 2003; Spoor et al., 2007) when compared to  
350 those of *P. quenstedti* (although when compared to more agile reptiles, all turtles possess short  
351 canals; Witmer et al., 2008).

352 Hearing was likely not well-developed in *P. quenstedti*, given the small overall size of the  
353 endosseous cochlear duct (Walsh et al., 2009) in comparison to other turtles. Even though its  
354 quadrate does not form the characteristic lateral round structure that encloses the cavum tympani in  
355 crown-turtles (Figures 4F–H), it possibly had a tympanic ear, similar to those of extant squamates  
356 and cheloniids, in which ~~it~~ the tympanum is supported by both bone and connective tissue (Henson,  
357 1974; Gaffney, 1990). However, the stapes of *P. quenstedti* was much stouter than that of crown-  
358 turtles (Figures 4D, E), and possibly articulated with the quadrate (Gaffney, 1990), suggesting that  
359 it was not as effective as the thin vibratory element characteristic of extant amniotes with tympanic  
360 hearing, including modern turtles (Baird, 1970; Clack, 1997). As proposed by Clack (1997) for  
361 diapsids, the elongation of the paraoccipital process of the opisthotic and its tight suture-suturing to  
362 the squamosal, ~~that~~ which occurred in the group including all testudinales but *Proganochelys*  
363 *quenstedti* (Sterli et al., 2010), may have completely released the stapes from its ancestral structural  
364 function (connecting the quadrate to other elements of the braincase) during turtle evolution.

365 The nasal cavity of *P. quenstedti* represents at least 42.2% of the total endocast volume  
366 (Table 1), fitting in the volume spectrum of terrestrial turtle taxa, which ranges from 29–43% in  
367 tortoises and 58.5–64% in meiolaniids (Carabajal et al., 2013). Larger nasal cavities have been  
368 related to occupation of arid environments, thermoregulation, sound-production or higher olfactory  
369 capabilities (Parsons, 1959, 1970; Paulina-Carabajal et al., 2017). In *P. quenstedti*, the cavum nasi  
370 proprium represents most of the volume of the nasal cavity and extends far dorsally and posteriorly.  
371 Within the nasal cavity, ~~Sensory-sensory~~ epithelium ~~on the nasal cavity~~ occurs only on the cavum  
372 walls (Parsons, 1970), and, as such, ~~its~~ the cavum's relative size could be used as a proxy for  
373 inferences ~~on~~ about olfactory capability in extinct reptiles. This connection, however, should be  
374 ~~taken-interpreted~~ cautiously, due to ~~its~~ the possible relation between cavum size and ~~to~~ other  
375 functions, such as thermoregulation or vocalization (Bourke et al., 2014; Paulina-Carabajal et al.,  
376 2017).

377 The size and volume of the olfactory bulbs have been shown to be related to a greater  
378 reliance on the olfactory sense in mammals and birds (Bang, 1971; Bang & Wenzel, 1985; Healy

and Guilford, 1990; Gittleman, 1991). In a series of studies the olfactory ratio (ratio between olfactory bulb and cerebral hemisphere maximum diameters; OR values) were used as a proxy to study ~~the~~ olfactory acuity and capacity in theropod dinosaurs (including birds) and crocodilians (Zelenitsky et al., 2009, 2011). More recently this has also been applied ~~for~~ to turtles (Paulina-Carabajal et al., 2017), showing that tortoises and meiolaniids (both terrestrial taxa) ~~show~~ have the highest OR values (36-62% and 20-45%, respectively). Even though OR may not be an exact measure of olfactory acuity it is currently the best available proxy and its use for a variety of reptilian taxa (Zelenitsky et al., 2009, 2011; Paulina-Carabajal et al., 2017) makes it a useful ~~comparable-comparative~~ metric. Here, we show that the OR is even higher in *P. quenstedti*, between 57-62% (Table 1), but in this case, these values may be also related to the less-developed cerebral hemispheres rather than to larger olfactory bulbs. Nevertheless, ~~its~~ the large nasal cavity in association with the high OR values supports our hypothesis that ~~the~~ olfaction was possibly the most developed sense in *P. quenstedti*.

### Evolution of the turtle brain endocast

~~As demonstrated by the results of~~ In the shape analysis, *Proganochelys quenstedti* is not contained in the morphospace occupied by any of the considered phylogenetic groups (Figure 5). There is extensive overlap in the PCA plots, but, at the same time, the PERMANOVA test shows a separation between Lepidosauromorpha, Testudinata and Archosauromorpha (Table 3). These results suggest that all amniotes (excluding dinosaurs and mammals) share a similar plesiomorphic brain endocast morphology, but that those lineages evolved in different directions in the morphospace.

Comparing general ecological groups (freshwater, marine, terrestrial and fossorial) provided similar results, with extensive overlap among the occupied morphospaces (Figure 6). *P. quenstedti* is contained in the morphospace occupied by the fossorial group ~~considering-on~~ the PC1/PC3 plot, but it falls outside every group on the other plots. Additionally, the statistical tests do not support significant differences between any of the considered groups (Table 3). On the other hand, the minimum spanning trees (see Supplementary Material) show that even when inside the fossorial morphospace *P. quenstedti* is ~~closer~~ closest to *Placodus*, a marine lepidosauromorph, and *Pseudopalatus*, an aquatic archosauromorph. A phylogenetic proximity to Sauropterygia (the lepidosauromorph lineage that includes *Placodus*) has been proposed previously (deBraga and Rieppel, 1997) and is associated ~~to~~ with the hypothesis that turtles originated in marine environments (Joyce and Gauthier, 2004; Joyce, 2015). The proximity of *P. quenstedti* and *Placodus* in our PC1/PC2 plot (Figure 6) may recall this hypothesis, but the poor sampling of

413 sauropterygians together with the extensive overlap between all groups (phylogenetic and  
414 ecological) cause us to refrain ~~us~~ from considering this a robust interpretation.

415 The shape analysis presented here is the first attempt to explore the evolution of  
416 neuroanatomy in amniotes with a quantitative approach. Even though our results do not support  
417 inferences about lifestyles from neuroanatomical data, the significant separation ~~of~~ between some of  
418 the considered phylogenetic groups (Figure 5, Table 3) seems promising. We can identify some  
419 caveats in our sample (e.g., few marine reptiles, synapsids and early amniotes) that can be easily  
420 overcome with the increasing use of computer tomography in paleontological and anatomical  
421 studies. Our approach using sagittal cross-section outlines could have also influenced the results,  
422 since there is a loss of information when the 3D endocast is simplified to a 2D outline.

423 More recently, Lyson et al. (2016) thoroughly analyzed the morphology of *Eumotosaurus*  
424 *africanus*, identifying some osteological correlates that led them to conclude that it was likely well-  
425 adapted for fossoriality. The authors also identified some of those correlates (e.g., large claws) in  
426 other proto- (e.g., *Odontochelys semitestacea*) and stem-turtles (*Proganochelys quenstedti* and  
427 *Palaeochersis talampayensis*), concluding that “fossoriality played an important role in the early  
428 evolution of turtles” (Lyson et al., 2016). Although in the PC1/PC3 plot (Figure 6) *P. quenstedti* is  
429 contained in the fossorial morphospace, the minimum spanning tree (see Supplementary Material)  
430 shows it to be closest to the terrestrial non-fossorial taxon *Chalarodon* and the statistical analyses  
431 do not support any significant differences between the considered groups (Table 3). While the shape  
432 analyses do not shed light on this problem conclusively, other sources of data are more convincing.  
433 *Proganochelys quenstedti* fossils were found in terrestrial-continental deposits (Gaffney, 1990) and  
434 analyses of forelimb proportions (Joyce and Gauthier, 2004) and paleohistology (Scheyer and  
435 Sander, 2007) support it as a terrestrial turtle. The morphology of its endosseous labyrinth with  
436 short semicircular canals oriented with at high angles to each other and the large cavum nasi  
437 proprium (Parsons, 1970; David et al., 2010; Paulina-Carabajal et al., 2017) agrees with these  
438 previous studies, strongly supporting the interpretation that *P. quenstedti* was a well-adapted  
439 terrestrial turtle. However, since its vestibule is not particularly large, in contrast to the condition of  
440 truly fossorial taxa (Yi and Norell, 2015) or of the semi-fossorial tortoise *Gopherus* (Paulina-  
441 Carabajal et al., 2017), we conclude the present data suggest it that it was likely not a fossorial  
442 taxon. In *P. quenstedti*, ~~the seemingly the relatively enlarged~~ vestibule in comparison to the other  
443 turtles in this study results from the relatively small semicircular canals. Thus, even if fossoriality  
444 had an important role during the early evolution of shell components (Lyson et al., 2016), our data  
445 suggests the complete turtle shell first appeared eds in a terrestrial taxon, with no evident link to  
446 fossoriality but most likely not fossorial turtle (i.e., at the Testudinata node).

Formatted: Font color: Auto

Formatted: Font color: Auto

Formatted: Font color: Auto, English (United States)

If we assume that the relatively simple morphology of *P. quenstedti* ~~more~~ closely resembles that of the testudinate ancestors, some trends can be inferred for the evolution of endocranial structures in turtles. An increase in overall encephalization, for example, with longer and more voluminous endocasts in relation to skull length is found already in the stem-turtle *Naomichelys speciosa* and ~~is extended~~ *continues* in crown-turtles (Figures 2, 3). Some regions became more pronounced as well. In *N. speciosa*, meiolaniids (Paulina-Carabajal et al., 2017), ~~as well as~~ *Plesiochelys etalloni* (Carabajal et al., 2013) and all other crown-turtles (Mautner et al., 2017; Ferreira et al., in press) the cerebral hemispheres are clearly distinguishable from the remainder of the endocast and ~~they~~ are wider in relation to skull and endocast length ~~when compared to~~ *than in* *P. quenstedti* (Figures 2, 3). The olfactory bulb can also be seen in the endocasts of some taxa, e.g., *Testudo graeca* and *Plesiochelys etalloni* (Carabajal et al., 2013; Paulina-Carabajal et al., 2017). However, this does not seem to be a general trend but rather one of the features that show noteworthy variations among crown-turtles, as are the degree of *development of the* cephalic and pontine inflexions and the sizes of the nasal cavity and the orbits. Considering that the brain of *P. quenstedti* was a simple tube-like structure with poorly differentiated regions, an increase in size and in regionalization of the brain took place later during the course of turtle evolution, similarly (although in a much lesser degree) to the trend observed during bird evolution (Balanoff et al., 2013), and achieved an endocast diversity comparable to other groups of amniotes, such as lepidosaurs and archosaurs (excluding dinosaurs; Figures 5, 6). Indeed, extant turtles possess high brain weights in relation to body weight, comparable to that of crocodiles (Gürtürkün et al. 2016), but that was not the ancestral condition of the group based on our analyses. ~~Given the recurrent results of phylogenetic analyses suggesting~~ *that turtles have* parareptilian affinity ~~of turtles~~ (e.g., Laurin and Piñeiro, 2017), it is important to sample the endocast diversity in that clade and explore the similarities between turtles and all other reptilian lineages. The simpler brain structure together with the large nasal cavity and nearly horizontal and short semicircular canals of the inner ear supports a picture of *P. quenstedti* as a terrestrial but most likely not fossorial turtle, with likely mediocre hearing and vision, but a well-developed olfactory sense.

**Acknowledgements.** We thank Daniela Schwarz for sharing the  $\mu$ CT-scan of the Berlin specimen, ~~and~~ Rainer Schoch for the ~~possibility~~ *permission* to  $\mu$ CT the Stuttgart specimen of *Proganochelys*. We thank Walter G. Joyce, Bill Simpson and Virginie Volpato for access to the specimens and CT scan data of *Naomichelys* and *Emys*. Adrian Tröscher, Jan Prochel, Irina Ruf and Kristin Mahlow are thanked for help with  $\mu$ CT-scans of extant species. We thank Gabe S. Bever and Walter G. Joyce for useful comments on a previous version of the manuscript ~~and the three anonymous~~

481 [reviewers that provided insightful comments and suggestions on the latest version of the](#)  
482 [manuscript.](#)

483  
484 **Author contribution statement.** Author contributions. S.L. and I.W. conceived and designed the  
485 study, S.L. performed the three-dimensional reconstruction, I.W. provided digital datasets, S.L.,  
486 G.S.F. and I.W. collected, analyzed and interpreted the data. S.L. and G.S.F. created figures and  
487 supplementary data. S.L., G.S.F. and I.W. contributed equally to the discussion, preparation and  
488 writing of the paper.

489  
490 **Competing interests statement:** There are no competing interests.

491  
492 **References**

493 Anderson, M.J. (2001). A new method for non-parametric multivariate analysis of variance. *Austral*  
494 *Ecol.* 26, 32–46.

495 Angielczyk, K.D., Burroughs, R.W., and Feldman, C. (2015). Do turtles follow the rules?  
496 Latitudinal gradients in species richness, body size, and geographic range area of the world's  
497 turtles. *J. Exp. Zool. B Mol. Dev. Evol.* 324, 270–294. doi:10.1002/jez.b.22602

498 ~~Anquetin, J. (2012). Reassessment of the phylogenetic interrelationships of basal turtles~~  
499 ~~(Testudinata). *J. Syst. Palaeontol.* 10, 3–45. doi:10.1080/14772019.2011.558928~~

500 Araújo, R., Fernandez, V., Polcyn, M.J., Fröbisch, J., and Martins, R.M. (2017). Aspects of  
501 gorgonopsian paleobiology and evolution: insights from the basicranium, occiput, osseous  
502 labyrinth, vasculature, and neuroanatomy. *PeerJ* 5, e3119. doi:10.7717/peerj.3119

503 Baird, I.L. (1970). “The anatomy of the reptilian ear,” in *Biology of the Reptilia*, eds. C. Gans and  
504 T.S. Parsons (Academic Press, London), 193–275.

505 ~~Balanoff, A. M., Bever, G. S., Colbert, M. W., Clarke, J. A., Field, D. J., Gignac, P. M., ... &~~  
506 ~~Walsh, S. (2016). Best practices for digitally constructing endocranial casts: examples from~~  
507 ~~birds and their dinosaurian relatives. *Journal of Anatomy*, 229(2), 173-190.~~

508 Bang, B.G. (1971). Functional anatomy of the olfactory system in 23 orders of birds. *Acta Anat.* 79,  
509 1–76. doi:10.1159/000143668

510 Bang, B.G., and Wenzel, B.M. (1985). “Nasal cavity and olfactory system,” in *Form and function*  
511 *in birds*, eds. A.S. King and J. McLelland (Academic Press, New York, NY), 195–225.

512 Bever, G.S., Lyson, T.R., Field, D.J., and Bhullar, B.-A.S. (2015). Evolutionary origin of the turtle  
513 skull. *Nature* 525,239–242. doi:10.1038/nature14900

Formatted: English (United States)

Formatted: English (United States)

Formatted: Font: 12 pt, Not Italic, Font color: Auto

Formatted: Font: 12 pt, Not Italic, Font color: Auto

Formatted: Font: 14 pt



514 Bhullar, B.-A.S., Bever, G.S. (2009). An Archosaur-Like Laterosphenoid in Early Turtles (Reptilia:  
515 Pantestudines). *Breviora* 518, 1–11.

516 Bona, P., and Paulina-Carabajal, A. (2013). *Caiman gasparinae* sp. nov., a huge alligatorid  
517 (Caimaninae) from the late Miocene of Paraná, Argentina. *Alcheringa* 37,1–12.  
518 doi:10.1080/03115518.2013.785335

519 Bourke, J.M., Ruger Porter, W.M., Ridgely, R.C., Lyson, T.R., Schachner, E.R., Bell, P.R., and  
520 Witmer, L.M. (2014). Breathing Life Into Dinosaurs: Tackling Challenges of Soft-Tissue  
521 Restoration and Nasal Airflow in Extinct Species. *Anat. Rec.* 297,2148–2186.  
522 doi:10.1002/ar.23046

523 Brichta, A., Acuna, D., and Peterson, E. (1988). Planar relations of semicircular canals in awake,  
524 resting turtles, *Pseudemys scripta*. *Brain Behav. Evolut.* 32,236–245.

525 Carabajal, A.P., Sterli, J., Müller, J., and Hilger, A. (2013). Neuroanatomy of the marine Jurassic  
526 turtle *Plesiochelys etalloni* (Testudinata, Plesiochelyidae). *PLoS One* 8, e69264.  
527 doi:10.1371/journal.pone.0069264

528 Clack, J. (1997). The evolution of tetrapod ears and the fossil record. *Brain Behav. Evolut.* 50, 198–  
529 212.

530 Claude, J., Pritchard, P.C., Tong, H., Paradis, E., and Auffray, J.-C. (2004). Ecological correlates  
531 and evolutionary divergence in the skull of turtles: a geometric morphometric assessment.  
532 *Syst. Biol.* 53,933–948.

533 Crampton, J.S., and Haines, A.J. (1996). Users' manual for programs Hangle, Hmatch and Hcurve  
534 for the Fourier shape analysis of two-dimensional outlines. *Institute of Geological and*  
535 *Nuclear Sciences, Science Report* 96, 1–28.

536 David, R., Droulez, J., Allain, R., Berthoz, A., Janvier, P., and Bennequin, D. (2010). Motion from  
537 the past. A new method to infer vestibular capacities of extinct species. *C. R. Palevol.* 9,  
538 397–410. doi:10.1016/j.crpv.2010.07.012

539 deBraga, M., and Rieppel, O. (1997). Reptile phylogeny and the interrelationships of turtles. *Zool.*  
540 *J. Linn. Soc.-Lond.* 120, 281–354.

541 DigiMorph. Digital Morphology - A unique biological visualization library.  
542 <http://www.digimorph.org/>. Last access 15.08.2017.

543 Edinger, T. (1942). The pituitary body in giant animals fossil and living: a survey and a suggestion.  
544 *Q. Rev. Biol.* 17, 31–45.

545 Ferreira, G.S., and Werneburg, I. (in press). “Evolution, diversity, and development of the  
546 craniocervical system in turtles with special reference to jaw musculature,” in *Heads, Jaws*

Formatted: Font color: Auto, English (United States)

Formatted: Font color: Auto, Portuguese (Brazil)

Formatted: Portuguese (Brazil)

Formatted: Font color: Auto, Portuguese (Brazil)

Formatted: Portuguese (Brazil)

Formatted: Font color: Auto, Portuguese (Brazil)

Formatted: Portuguese (Brazil)



and Muscles – Evolution, development, anatomical diversity and function, eds. J. Ziermann, R.R. Diaz Jr, and R. Diogo (Springer, Heidelberg).

Ferreira, G.S., Iori, F.V., Hermanson, G., and Langer, M.C. (in press). New turtle remains from the Late Cretaceous of Monte Alto-SP, Brazil, including cranial osteology, neuroanatomy and phylogenetic position of a new taxon. *Paläontol. Zeit.*

Field, D.J., Gauthier, J.A., King, B.L., Pisani, D., Lyson, T.R., and Peterson, K.J. (2014). Toward consilience in reptile phylogeny: miRNAs support an archosaur, not lepidosaur, affinity for turtles. *Evol. Dev.* 16, 189–196. doi:10.1111/ede.12081

Foth, C., and Joyce, W.G. (2016). Slow and steady: the evolution of cranial disparity in fossil and recent turtles. *P. Roy. Soc. Lond. B Bio.* 283m 20161881. doi:10.1098/rspb.2016.1881

Foth, C., Rabi, M., and Joyce, W.G. (2017). Skull shape variation in extant and extinct Testudinata and its relation to habitat and feeding ecology. *Acta Zool.-Stockholm* 98, 310–325. doi:10.1111/azo.12181

Franzosa, J.W. (2004). Evolution of the brain in Theropoda (Dinosauria). [PhD dissertation]. [Austin (TX)]: University of Texas.

Gaffney, E.S. (1979). Comparative cranial morphology of Recent and fossil turtles. *B. Am. Mus. Nat. Hist.* 164, 65–376.

Gaffney, E.S. (1982). Cranial morphology of the baenid turtles. *Am. Mus. Novit.* 2737, 1–22.

Gaffney, E.S. (1990). The comparative osteology of the Triassic turtle *Proganochelys*. *B. Am. Mus. Nat. Hist.* 194, 1–263.

Gaffney, E.S. (1996). The postcranial morphology of *Meiolania platyceps* and a review of the Meiolaniidae. *B. Am. Mus. Nat. Hist.* 229, 1–166.

Gaffney, E.S., and Zangerl, R. (1968). *A Revision of the Chelonian Genus Bothremys: (Pleurodira: Pelomedusidae)*. Chicago: Field Museum of Natural History.

~~Gaffney, E.S., Meylan, P.A., and Wyss, A.R. (1991). A computer-assisted analysis of the relationships of the higher categories of turtles. *Cladistics* 7, 313–335.~~

Gauthier, J.A., Kluge, A.G., and Rowe, T. (1988). “The early evolution of the Amniota,” in *The phylogeny and classification of the tetrapods*, vol. 1, ed. M.J. Benton (Oxford: Oxford University Press) 103–155.

George, I.D., and Holliday, C.M. (2013). Trigeminal nerve morphology in *Alligator mississippiensis* and its significance for crocodyliform facial sensation and evolution. *Anat. Rec.* 296, 670–680. doi:10.1002/ar.22666

Gittleman, J.L. (1991). Carnivore olfactory bulbs: allometry, phylogeny and ecology. *J. Zool.* 225, 253–272.

- Guillon, J.-M., Guéry, L., Hulin, V., and Girondot, M. (2012). A large phylogeny of turtles (Testudines) using molecular data. *Contrib. Zool.* 81, 147–158.
- ~~Güntürkün, O., Stacho, M., and Ströckens, F. (2016). "The brains of reptiles and birds," in *Evolution of Nervous Systems – the evolution of the nervous systems in nonmammalian vertebrates*, vol. 1, ed. J.H. Kaas (Oxford: Academic Press), 171–221.~~
- Haines, A.J., and Crampton, J.S. (2000). Improvements to the method of Fourier shape analysis as applied in morphometric studies. *Palaeontology*, 43, 765–783.
- Halpern, M. (1992). "Nasal chemical senses in reptiles," in *Biology of the Reptilia*, vol. 18, eds. C. Gans, and D. Crews (Chicago and London: University of Chicago Press), 423–523.
- Hammer, Ø., Harper, D.A.T., and Ryan, P.D. (2001). Past: Paleontological Statistics Software Package for Education and Data Analysis. *Palaeontol. Electron.* 4, 1–9.
- Healy, S. and Guilford, T. (1990). Olfactory-bulb size and nocturnality in birds. *Evolution* 44, 339–346. doi:10.2307/2409412.
- Hedges, S.B., and Poling, L.L. (1999). A molecular phylogeny of reptiles. *Science* 283, 998–1001.
- Henson Jr, O. (1974). "Comparative anatomy of the middle ear," in *Auditory System*, eds. W.D. Keidel, and W.D. Neff (Berlin: Springer Verlag), 39–110.
- Herrel, A., Van Damme, J., and Aerts, P. (2008). „Cervical anatomy and function in turtles," in *Biology of Turtles*, eds. J. Wyneken, M.H. Godfrey, and V. Bels (New York: CRC Press,., 163–185.
- Herrera, Y., Fernández, M.S., and Gasparini, Z. (2013). The snout of *Cricosaurus araucanensis*: a case study in novel anatomy of the nasal region of metriorhynchids. *Lethaia* 46, 331–340. doi:10.1111/let.12011
- Holloway, W.L., Claeson, K.M., and O'Keefe, F.R. (2013). A virtual phytosaur endocast and its implications for sensory system evolution in archosaurs. *J. Vertebr. Paleontol.* 33, 848–857. doi:10.1080/02724634.2013.747532
- Hopson, J.A. (1979). "Palaeoneurology," in *Biology of the reptilia*, vol. 9, ed. C. Gans (New York: Academic Press), 39–146.
- Jaekel, O. (1918). Die Wirbeltierfunde aus dem Keuper von Halberstadt. Serie II. Testudinata. Teil 1. *Stegochelys dux*, n.g., n.sp. *Paläontol. Zeit.* 2, 88–214.
- Jirak, D., and Janacek, J. (2017). Volume of the crocodilian brain and endocast during ontogeny. *PLoS One* 12, e0178491. doi:10.1371/journal.pone.0178491
- Joyce, W.G. (2015). The origin of turtles: a paleontological perspective. *J. Exp. Zool. B Mol. Dev. Evol.* 324, 181–193. doi:10.1002/jez.b.22609

Formatted: Font color: Auto, English (United States)

Formatted: Font color: Auto, German (Germany)

614 Joyce, W.G., and Gauthier, J.A. (2004). Palaeoecology of Triassic stem turtles sheds new light on  
615 turtle origins. *P. Roy. Soc. Lond. B Bio.* 271, 1–5.

616 Joyce, W.G., Parham, J.F., and Gauthier, J.A. (2004). Developing a protocol for the conversion of  
617 rank-based taxon names to phylogenetically defined clade names, as exemplified by turtles.  
618 *J. Paleontol.* 78, 989–1013.

619 Joyce, W.G., Rabi, M., Clark, J.M., and Xu, X. (2016). A toothed turtle from the Late Jurassic of  
620 China and the global biogeographic history of turtles. *BMC Evol. Biol.* 16, 236.  
621 doi:10.1186/s12862-016-0762-5

622 Laaß, M., Schillinger, B., and Kaestner, A. (2017). What did the "unossified zone" of the non-  
623 mammalian therapsid braincase house? *J. Morphol.* 278, 1020–1032.  
624 doi:10.1002/jmor.20583

625 Laurin, M., and Piñeiro, G.H. (2017). A reassessment of the taxonomic position of mesosaurs, and a  
626 surprising phylogeny of early amniotes. *Front. Earth Sci.* 5: 88. doi:  
627 10.3389/feart.2017.00088.

628 Lautenschlager, S. (2014a). Morphological and functional diversity in therizinosaur claws and the  
629 implications for theropod claw evolution. *P. Roy. Soc. Lond. B Bio.* 281, 20140497.  
630 doi:10.1098/rspb.2014.0497

631 Lautenschlager, S. (2014b). Palaeontology in the third dimension: a comprehensive guide for the  
632 integration of three-dimensional content in publications. *Paläontol. Zeit.* 88, 111–121.  
633 doi:10.1007/s12542-013-0184-2

634 Lautenschlager S, Butler RJ. 2016. Neural and endocranial anatomy of Triassic phytosaurian  
635 reptiles and convergence with fossil and modern crocodylians. *PeerJ* 4:e2251.  
636 doi:10.7717/peerj.2251

637 Lee, M.S. (1997). Reptile relationships turn turtle. *Nature* 389, 245–245.

638 Li, C., Wu, X.-C., Rieppel, O., Wang, L.-T., and Zhao, L.-J. (2008). An ancestral turtle from the  
639 Late Triassic of southwestern China. *Nature* 456, 497–501. doi:10.1038/nature07533

640 Liu, J., Rieppel, O., Jiang, D.-Y., Aitchison, J.C., Motani, R., Zhang, Q.-Y., Zhou, C.-Y., and Sun,  
641 Y.-Y. (2011). A new pachypleurosauros (Reptilia: Sauropterygia) from the Lower Middle  
642 Triassic of Southwestern China and the phylogenetic relationships of Chinese  
643 pachypleurosauros. *J. Vertebr. Paleontol.* 85, 32–36.

644 Lyson, T.R., Bever, G.S., Bhullar, B.-A.S., Joyce, W.G., and Gauthier, J.A. (2010). Transitional  
645 fossils and the origin of turtles. *Biol. Letters.* rsbl20100371. doi:10.1098/rsbl.2010.0371

646 Lyson, T.R., Rubidge, B.S., Scheyer, T.M., de Queiroz, K., Schachner, E.R., Smith, R.M.H., Botha-  
 647 Brink, J., and Bever, G.S. (2016). Fossorial origin of the turtle shell. *Curr. Biol.* 26, 1887–  
 648 1894. doi:10.1016/j.cub.2016.05.020  
 649 Mautner, A.K., Latimer, A.E., Fritz, U., and Scheyer, T.M. (2017). An updated description of the  
 650 osteology of the pancake tortoise *Malacochersus tornieri* (Testudines: Testudinidae) with  
 651 special focus on intraspecific variation. *J. Morphol.* 278, 321–333. doi:10.1002/jmor.20640  
 652 Neenan, J.M., and Scheyer, T.M. (2012). The braincase and inner ear of *Placodus gigas*  
 653 (Sauropterygia, Placodontia)-a new reconstruction based on micro-computed tomographic  
 654 data. *J. Vertebr. Paleontol.* 32, 1350–1357. doi:10.1080/02724634.2012.695241  
 655 Neenan, J.M., Klein, N., and Scheyer, T.M. (2013). European origin of placodont marine reptiles  
 656 and the evolution of crushing dentition in Placodontia. *Nat. Commun.* 4, 1621.  
 657 doi:10.1038/ncomms2633  
 658 Parsons, T.S. (1959). Nasal anatomy and the phylogeny of reptiles. *Evolution* 13, 175–187  
 659 Parsons, T.S. (1970). “The Nose and Jacobson’s Organ,” in *Biology of the Reptilia*, Vol. 2B, ed. C.  
 660 Gans (New York: Academic Press), 99–191.  
 661 Paulina-Carabajal, A., Sterli, J., Georgi, J., Poropat, S.F., and Kear, B.P. (2017). Comparative  
 662 neuroanatomy of extinct horned turtles (Meiolaniidae) and extant terrestrial turtles  
 663 (Testudinidae), with comments on the palaeobiological implications of selected endocranial  
 664 features. *Zool. J. Linn. Soc.-Lond.* zlw024. doi:10.1093/zoolinnean/zw024  
 665 Pierce, S.E., Williams, M., and Benson, R.B. (2017). Virtual reconstruction of the endocranial  
 666 anatomy of the early Jurassic marine crocodylomorph *Pelagosaurus typus* (Thalattosuchia).  
 667 *PeerJ* 5, e3225. doi:10.7717/peerj.3225  
 668 Poglayen-Neuwall, I. (1953). Untersuchungen der Kiefermuskulatur und deren Innervation bei  
 669 Schildkröten. *Acta Zool.-Stockholm* 34, 241–292.  
 670 Rieppel, O. (2007). “The Relationships of Turtles within Amniotes,” in *Biology of turtles: from*  
 671 *structures to strategies of life*, eds. J. Wyneken, M.H. Godfrey, and V. Bels (Boca Raton:  
 672 CRC Press), 345–353.  
 673 Rieppel, O. (2013). “The evolution of the turtle shell,” in *Morphology and evolution of turtles*, eds.  
 674 D.B. Brinkman, P.A. Holroyd, and J.D. Gardner (Heidelberg: Springer), 51–61.  
 675 doi:10.1007/978-94-007-4309-0\_5  
 676 Rieppel, O., and Reisz, R.R. (1999). The origin and early evolution of turtles. *Annu. Rev. Ecol. Syst.*  
 677 30, 1–22.  
 678 Rohlf, F. (2010). *TPSDig2, version 2.16*. New York: Stony Brook.

679 Scheyer, T.M., Neenan, J.M., Bodogan, T., Furrer, H., Obrist, C., and Plamondon, M. (2017). A  
 680 new, exceptionally preserved juvenile specimen of *Eusaurosphargis dalsassoi* (Diapsida)  
 681 and implications for Mesozoic marine diapsid phylogeny. *Sci. Rep.* 7, 4406.  
 682 doi:10.1038/s41598-017-04514-x  
 683 Scheyer, T.M., and Sander, P.M. (2007). Shell bone histology indicates terrestrial palaeoecology of  
 684 basal turtles. *P. Roy. Soc. Lond. B Bio.* 274, 1885–1893. doi:10.1098/rspb.2007.0499  
 685 Schoch, R.R., and Sues, H.-D. (2015). A Middle Triassic stem-turtle and the evolution of the turtle  
 686 body plan. *Nature* 523, 584–587. doi:10.1038/nature14472  
 687 Schoch, R.R., and Sues, H.-D. (2017). Osteology of the Middle Triassic stem-turtle *Pappochelys*  
 688 *rosinae* and the early evolution of the turtle skeleton. *J. Syst. Palaeontol.*  
 689 doi:10.1080/14772019.2017.1354936  
 690 Schumacher, G.H. (1973). “The head muscles and hyolaryngeal skeleton of turtles and  
 691 crocodilians,” in *Biology of the Reptilia*, eds. C. Gans, and T.S. Parsons (London and New  
 692 York: Academic Press), 101–200.  
 693 Spoor, F. (2003). The semicircular canal system and locomotor behaviour, with special reference to  
 694 hominin evolution. *Courier-Forschungsinstitut Senckenberg* 93-104.  
 695 Spoor, F., Garland, T., Krovitz, G., Ryan, T.M., Silcox, M.T., and Walker, A. (2007). The primate  
 696 semicircular canal system and locomotion. *P. Acad. Nat. Sci. Phila.* 104, 10808–10812.  
 697 doi:10.1073/pnas.0704250104  
 698 Sterli, J., Müller, J., Anquetin, J., and Hilger, A. (2010). The parabasisphenoid complex in  
 699 Mesozoic turtles and the evolution of the testudinate basicranium. *Can. J. Earth Sci.* 47,  
 700 1337–1346. doi:10.1139/E10-061  
 701 von Baczko, M.B., and Desojo, J.B. (2016). Cranial Anatomy and Palaeoneurology of the  
 702 Archosaur *Riojasuchus tenuisiceps* from the Los Colorados Formation, La Rioja, Argentina.  
 703 *PLoSOne* 11, e0148575. doi:10.1371/journal.pone.0148575  
 704 Walsh, S.A., Barrett, P.M., Milner, A.C., Manley, G., and Witmer, L.M. (2009). Inner ear anatomy  
 705 is a proxy for deducing auditory capability and behaviour in reptiles and birds. *P. Roy. Soc.*  
 706 *Lond. B Bio.* 276, 1355–1360. doi:10.1098/rspb.2008.1390  
 707 Wang, Z., Pascual-Anaya, J., Zadissa, A., Li, W., Niimura, Y., Huang, Z., Li, C., White, S., Xiong,  
 708 Z., Fang, D. (2013). The draft genomes of soft-shell turtle and green sea turtle yield insights  
 709 into the development and evolution of the turtle-specific body plan. *Nat. Genet.* 45, 701–  
 710 706. doi:10.1038/ng.2615  
 711 Werneburg, I. (2011). The cranial musculature of turtles. *Palaeontol. Electron.* 14, 1–99.  
 712 doi:10.5167/uzh-48569

713 Werneburg, I. (2013). Jaw musculature during the dawn of turtle evolution. *Org. Divers. Evol.* 13,  
 714 225-254. doi:10.1007/s13127-012-0103-5

715 Werneburg, I. (2015). Neck motion in turtles and its relation to the shape of the temporal skull  
 716 region. *C. R. Palevol* 14, 527–548. doi:10.1016/j.crpv.2015.01.007

717 Werneburg, I., and Sánchez-Villagra, M.R. (2009). Timing of organogenesis support basal position  
 718 of turtles in the amniote tree of life. *BMC Evol. Biol.* 9, 82. doi:10.1186/1471-2148-9-82

719 Werneburg, I., Hinz, J.K., Gumpenberger, M., Volpato, V., Natchev, N., and Joyce, W.G.. 2015a.  
 720 Modeling neck mobility in fossil turtles. *J. Exp. Zool. B Mol. Dev. Evol.* 324, 230–243.  
 721 doi:10.1002/jez.b.22557

722 Werneburg, I., Wilson, L.A., Parr, W.C., and Joyce, W.G. (2015b). Evolution of Neck Vertebral  
 723 Shape and Neck Retraction at the Transition to Modern Turtles: an Integrated Geometric  
 724 Morphometric Approach. *Syst. Biol.* 64, 187–204. doi:10.1093/sysbio/syu072

725 Witmer, L.M., Ridgely, R.C., Dufeu, D.L., and Semones, M.C. (2008). “Using CT to Peer into the  
 726 Past: 3D Visualization of the Brain and Ear Regions of Birds, Crocodiles, and Nonavian  
 727 Dinosaurs,” in *Anatomical imaging*, eds. H. Endo, and R. Frey (Tokyo: Springer), 67–87.

728 Yi, H., and Norell, M.A. (2015). The burrowing origin of modern snakes. *Sci. Adv.* 1, e1500743.  
 729 doi: 10.1126/sciadv.1500743

730 Zangerl, R.A. (1960). A new specimen of *Desmatochelys lowii* Williston; a primitive sea turtle  
 731 from the Cretaceous of South Dakota. *Fieldiana, Geology* 14, 7–40.

732 Zelenitsky, D.K., Therrien, F., and Kobayashi, Y. (2009). Olfactory acuity in theropods:  
 733 palaeobiological and evolutionary implications. *Proc. R. Soc. B.* 276, 667-673.

734 Zelenitsky, D.K., Therrien, F., Ridgely, R.C., McGee, A.R., and Witmer, L.W. (2011). Evolution of  
 735 olfaction in non-avian theropod dinosaurs and birds. *Proc. R. Soc. B.* 278, 3625–3634.  
 736 doi:10.1098/rspb.2008.1075

737

Formatted: Portuguese (Brazil)

738 **Tables**

739 **Table 1. Measurements and ratios for sampled taxa.** ASC-PSC, angle between anterior and  
740 posterior semicircular canals; BL, basicranial length; CE/BL, cubic root of endocast  
741 volume/basicranial length; CE/SL, cubic root of endocast volume/skull length; EV, endocast  
742 volume; NV, nasal cavity volume; N/E, nasal cavity/endocast volume ratio; OR, olfactory ratio; SL,  
743 skull length.

Taxon	Specimen ID	SL [mm]	BL [mm]	EV [mm <sup>3</sup> ]	NV [mm <sup>3</sup> ]	N/E	CE/SL	CE/BL	OR [%]	ASC-PSC
<i>Proganochelys</i>	MB1910.45.2	175	148.75	8170.84	12209.34	1.49	11.51	13.54	62.5	107°
<i>Proganochelys</i>	SMNS 16980	97	85.36	3790.56	3709.39	0.98	16.07	18.27	57.14	-
<i>Naomichelys</i>	FMNH PR273	117	103.50	9805.97	4077.77	0.42	18.29	20.68	15-19	79°
<i>Podocnemis</i>	SMF 55470	67	51.32	1732.45	531.57	0.31	17.93	23.40	13.39	81°
<i>Chelodina</i>	ZMB H 49659	36	36.00	760.10	140.84	0.18	25.35	25.35	11.34	98°
<i>Chelonia</i>	ZMB 37416 MS	112	80.64	7077.93	2667.23	0.38	17.14	23.81	31.65	94°
<i>Macrochelys</i>	GPIT/RE/10801	120	105.88	9583.53	3568.33	0.37	17.70	20.06	38.18	88°
<i>Platysternon</i>	SMF 69684	60	46.43	898.13	314.33	0.35	16.08	20.78	28.23	82°
<i>Malacochersus</i>	SMF 58702	35	40.92	1364.13	669.45	0.49	31.69	27.11	16.06	86°
<i>Emys</i>	WGJ 1987a	31	30.42	668.07	118.54	0.18	28.20	28.74	17.31	102°
<i>Emydura</i>	PIMUZ 2009.37	35	35.00	1556.29	160.65	0.10	33.11	33.11	9.80	90°
<i>Pelodiscus</i>	IW576-2	59	39.48	707.23	444.09	0.63	15.10	22.57	20.25	79°

744

745

746 **Table 2.** Summary of the results of the principal component analyses of the brain outlines of  
 747 different turtles specimens of turtles and other groups. Summary of the results of the Principal  
 748 Component Analyses.

Formatted: Font color: Auto

Formatted: Font color: Auto

PC	Eigenvalue	% variance	% cumulative variance
1	0.01042	41.4	41.4
2	0.00464	18.5	59.9
3	0.00298	11.8	71.7
4	0.00174	6.9	78.7
5	0.00137	5.5	84.1
6	0.00093	3.7	87.8
7	0.00067	2.6	90.5
8	0.00042	1.7	92.1
9	0.00032	1.3	93.4
10	0.00028	1.1	94.5
11	0.00021	0.8	95.4

749  
750

In review



**Table 3.** Results of one-way PERMANOVA test (10000 permutations) with 95% of variance (PC1-PC11), excluding *Proganochelys* and *Diadectes* (for phylogenetic groups only).

Phylogenetic groups			
Permutation N	10000		
Total sum of squares (SQ)	1,901		
Within-group SQ	1,599		
F	3,653		
p	1.00E-01		
	Testudinata	Archosauromorpha	Lepidosauromorpha
Testudinata			
Archosauromorpha	0.8423		
Lepidosauromorpha	0.003	0.0005999	
Synapsida	0.327	0.1056	0.4488
Ecological groups			
Permutation N	10000		
Total SQ	77		
Within-group SQ	72		
F	1		
p	0.1656		
	Terrestrial	Aquatic	Marine
Terrestrial			
Aquatic	1		
Marine	0.252	1	
Fossorial	0.6485	1	0.8387

**Figures**

**Figure 1. Endocranial anatomy of *Proganochelys quenstedti* specimens (A-D) MB 1910.45.2 and (E-H) SMNS 16980.** Endocast and nasal cavity (A, B) *in situ* in left lateral oblique view with bone rendered semi-transparent and isolated endocast in (B, F) left lateral, (C, G) dorsal and (D, H) ventral views. Abbreviations: car, carotid artery; [duc, ductus nasopharyngeus](#); dur, dural peak; endo, brain endocast; lab, endosseous labyrinth; nas, endocast of nasal cavity; pit, pituitary fossa; I, olfactory nerve; II, optic nerve canal; oculomotor nerve canal; IV, trochlear nerve canal; V, trigeminal nerve canal; VI, abducens nerve canal; VII, facial nerve canal; IX-XI shared canal for the glossopharyngeal, vagus and spinal accessory nerve; XII, hypoglossal nerve canal.

764  
765  
766  
767  
768  
769  
770  
771  
772  
773  
774  
775  
776  
777  
778  
779  
780  
781  
782  
783  
784  
785  
786  
787  
788  
789  
790  
791  
792  
793  
794  
795  
796  
797  
798

**Figure 2. Comparative endocranial anatomy of different stem-Testudines and pleurodiran taxa.** Original reconstructions and redrawn endocasts (*Plesiobaena antiqua* from Gaffney, 1982; *Meiolania platyceps* from Paulina-Carabajal et al., 2017; *Yuraramirim montealtensis* from Ferreira et al., in press) in left lateral view. Topology based on Joyce et al. (2016), Guillon et al. (2012) and Ferreira et al. (in press). Heat mapping on branches based on the ratio (CE/BL) between cubic root of endocast volume and basicranial length (Table 1).

**Figure 3. Comparative endocranial anatomy of different pan-cryptodiran taxa.** Original reconstructions and redrawn endocasts (*Plesiochelys etalloni* from Carabajal et al., 2013; *Gopherus berlandieri* from Paulina-Carabajal et al., 2017) in left lateral view. Topology based on Joyce et al. (2016), and Guillon et al. (2012). Heat mapping on branches based on the ratio (CE/BL) between cubic root of endocast volume and basicranial length (Table 1).

**Figure 4. Inner ear and otic region anatomy of *Proganochelys quenstedti*.** Digital reconstruction of the right endosseus labyrinth of *P. quenstedti* in (A) right lateral, (B) dorsal, and (C) anterior views. Skulls of (D) *P. quenstedti* and (E) *Eubaena cephalica* in posterior view, redrawn from Gaffney (1990) with opisthotic and stapes colored in green and blue, respectively. Skulls of (F) *Sphenodon punctatus*, (G) *Emydura macquarii*, and (H) *P. quenstedti* in lateral view, redrawn from Ferreira & Werneburg (in press), with quadrate colored in red. Note the larger proportions of the stapes and its contact with the quadrate bone in *P. quenstedti*, and its slender and tall quadrate, similar to that of *S. punctatus*, and distinct from the round one of other turtles, ~~that which~~ completely encloses the tympanic membrane. Abbreviations: asc, anterior semicircular canal; cc, crus communis; ex, exoccipital; fo, fenestra ovalis; lsc, lateral semicircular canal; pa, parietal; psc, posterior semicircular canal; qu, quadrate; sq, squamosal; ves, vestibulum.

**Figure 5. Two dimensional morphospace plots of brain endocast outlines based on the first three PC axes** using a priori defined phylogenetic groups. *Diadectes* is shown as a black cross, *Proganochelys quenstedti* (SMNS 16980) in bold. The symbols are used to identify the clade to which a point was assigned. Different vertebrate groups are indicated by convex hulls.

**Figure 6. Two dimensional morphospace plots of brain endocast outlines based on the first three PC axes** using a priori defined ecological groups. *Diadectes* is shown as a black cross, *Proganochelys quenstedti* (SMNS 16980) in bold. The symbols are used to identify the clade to which a point was assigned. Different vertebrate groups are indicated by convex hulls.

Formatted: Font: Not Italic  
Formatted: Font: Not Italic

Formatted: Font color: Auto

799

800 **Figure 7.** Overall skull shape and ~~proportional~~ relation to cranial structures in different turtle taxa.  
801 Brain endocast and adductor chamber plotted in left lateral (first and third rows) and dorsal (second  
802 and fourth rows) views. Note the similar position of the trigeminal nerve exit regardless of ~~the~~  
803 changes in surrounding structures.

In review

Figure 1.JPEG

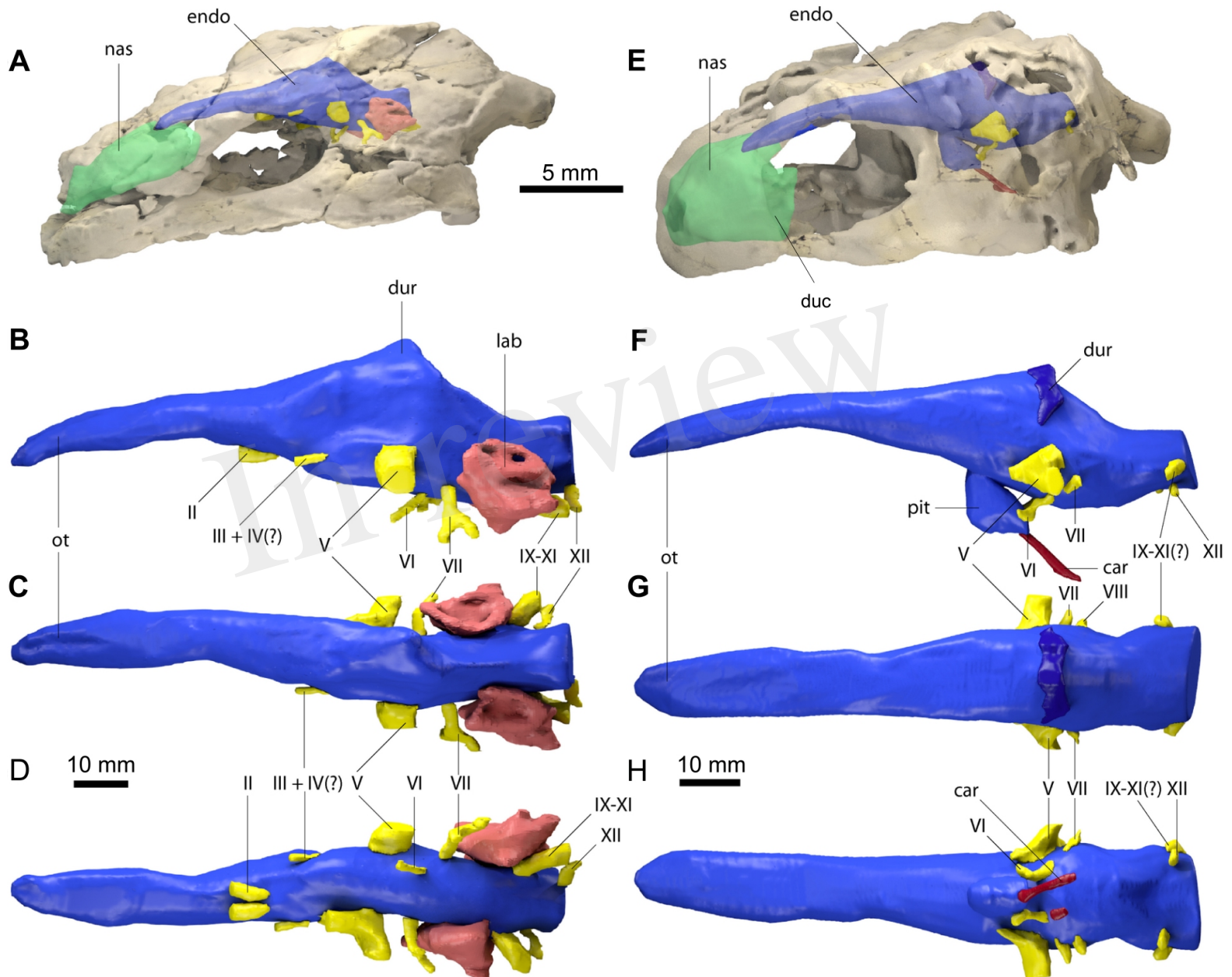
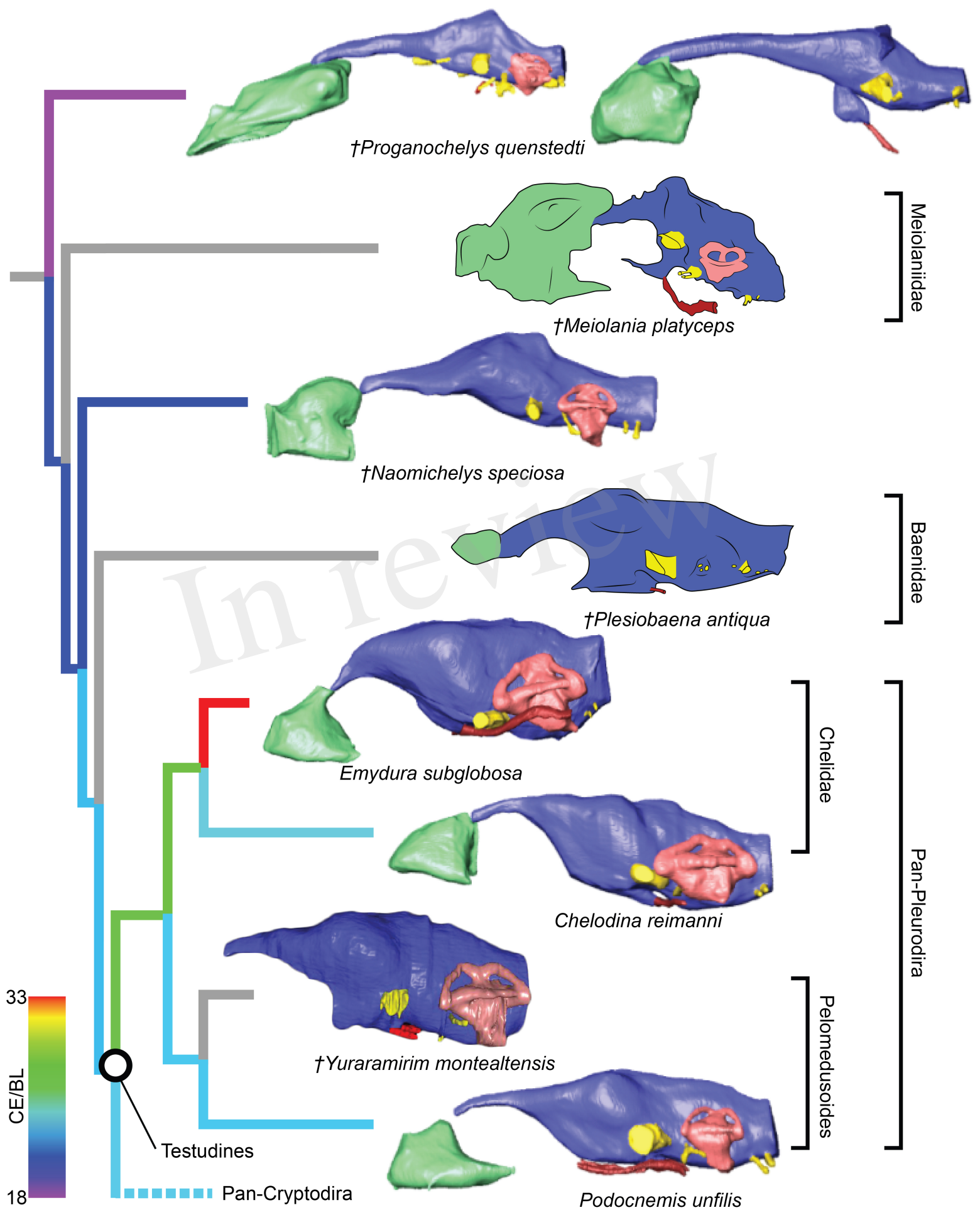
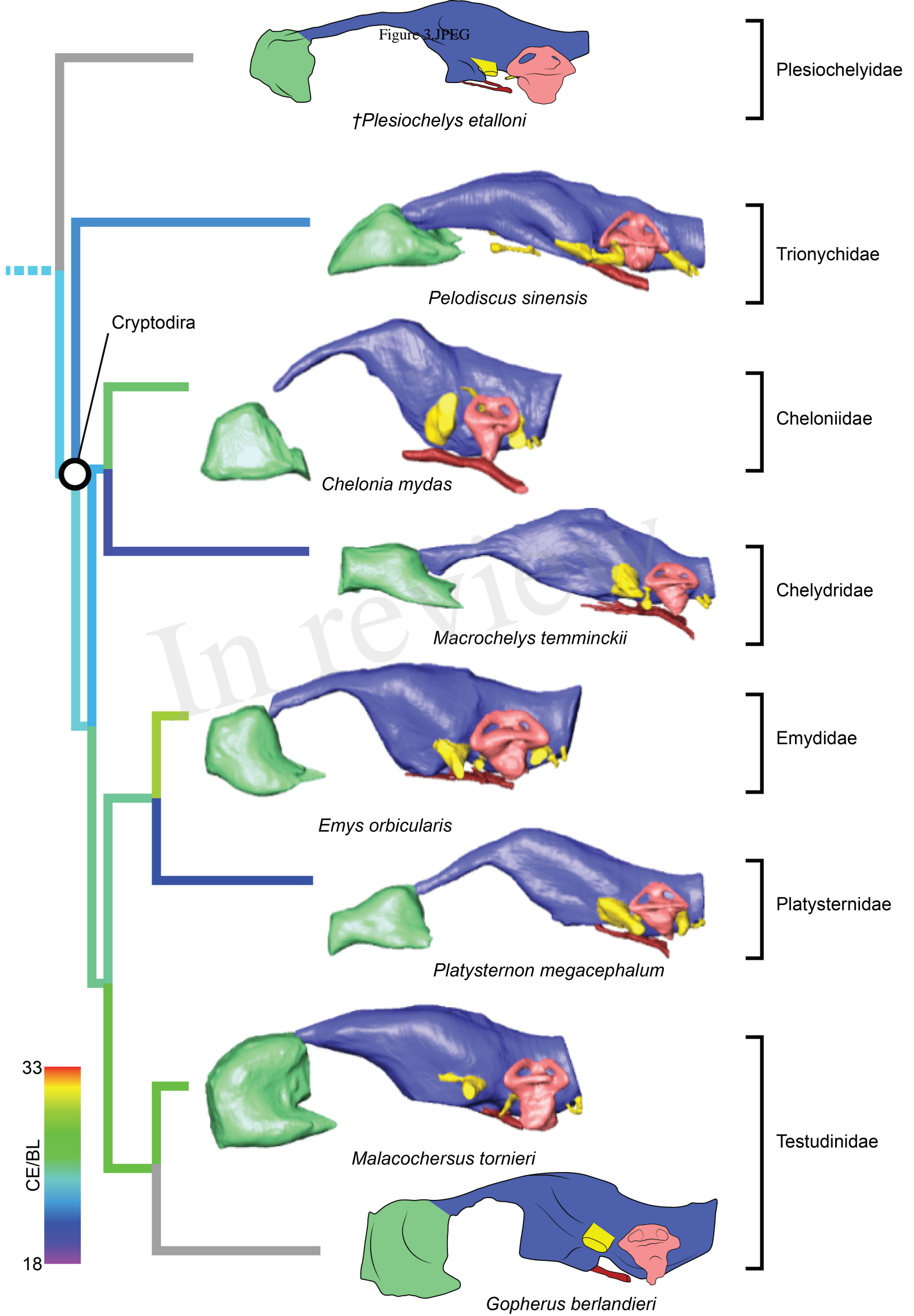
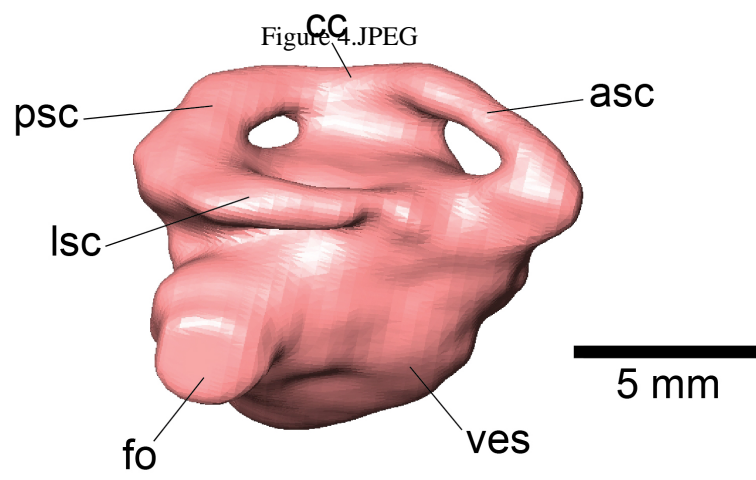
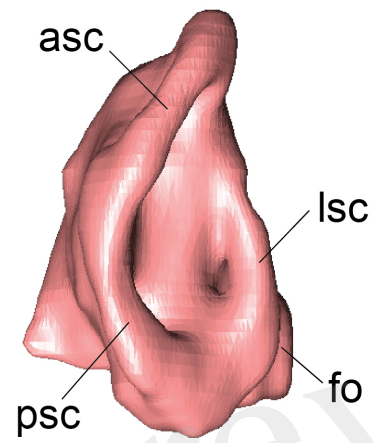
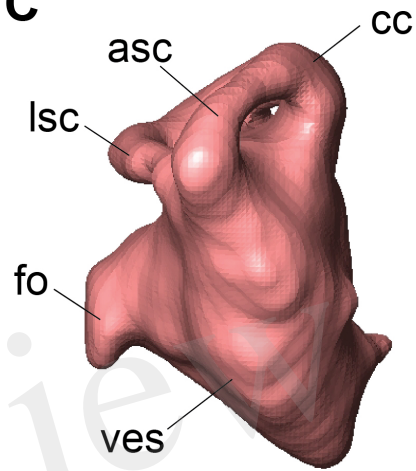
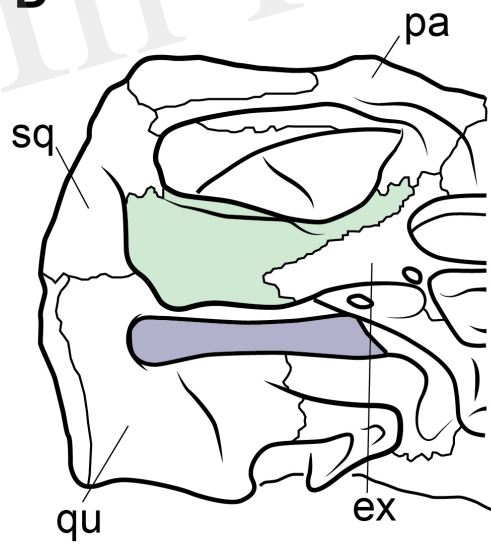
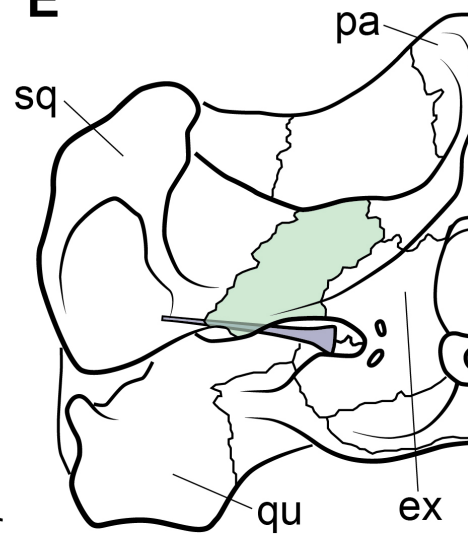
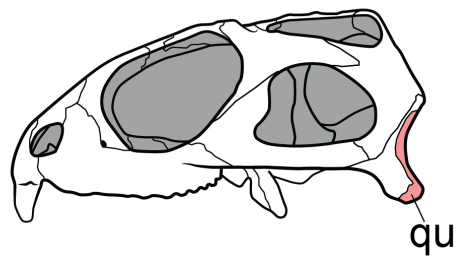
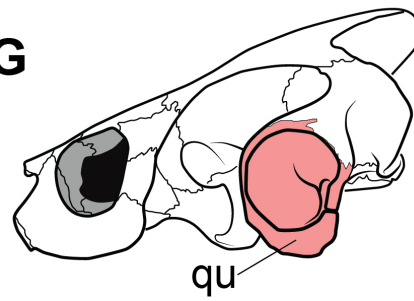
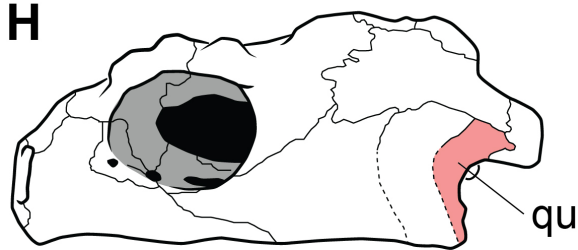


Figure 2.JPEG







**A****B****C****D****E****F****G****H**





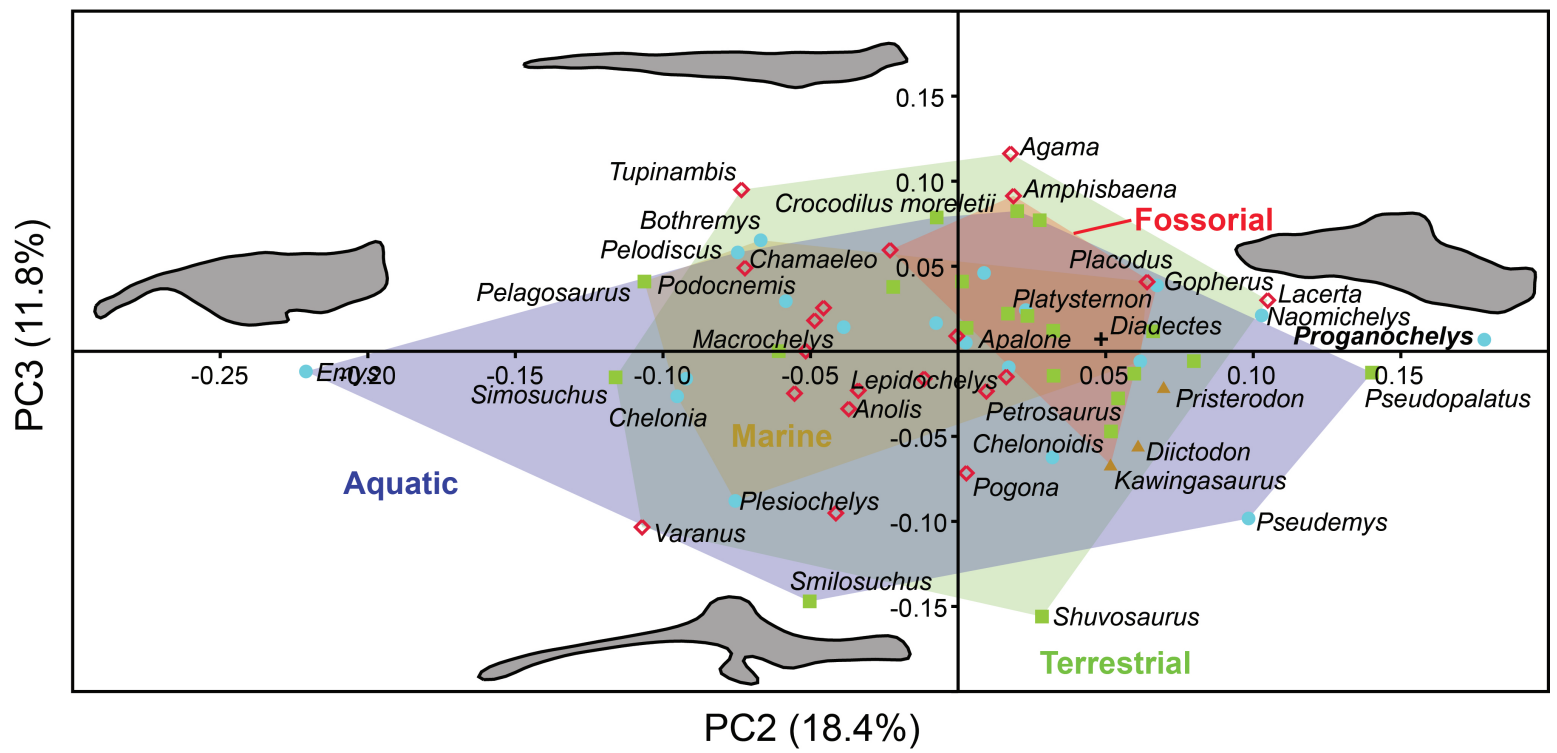
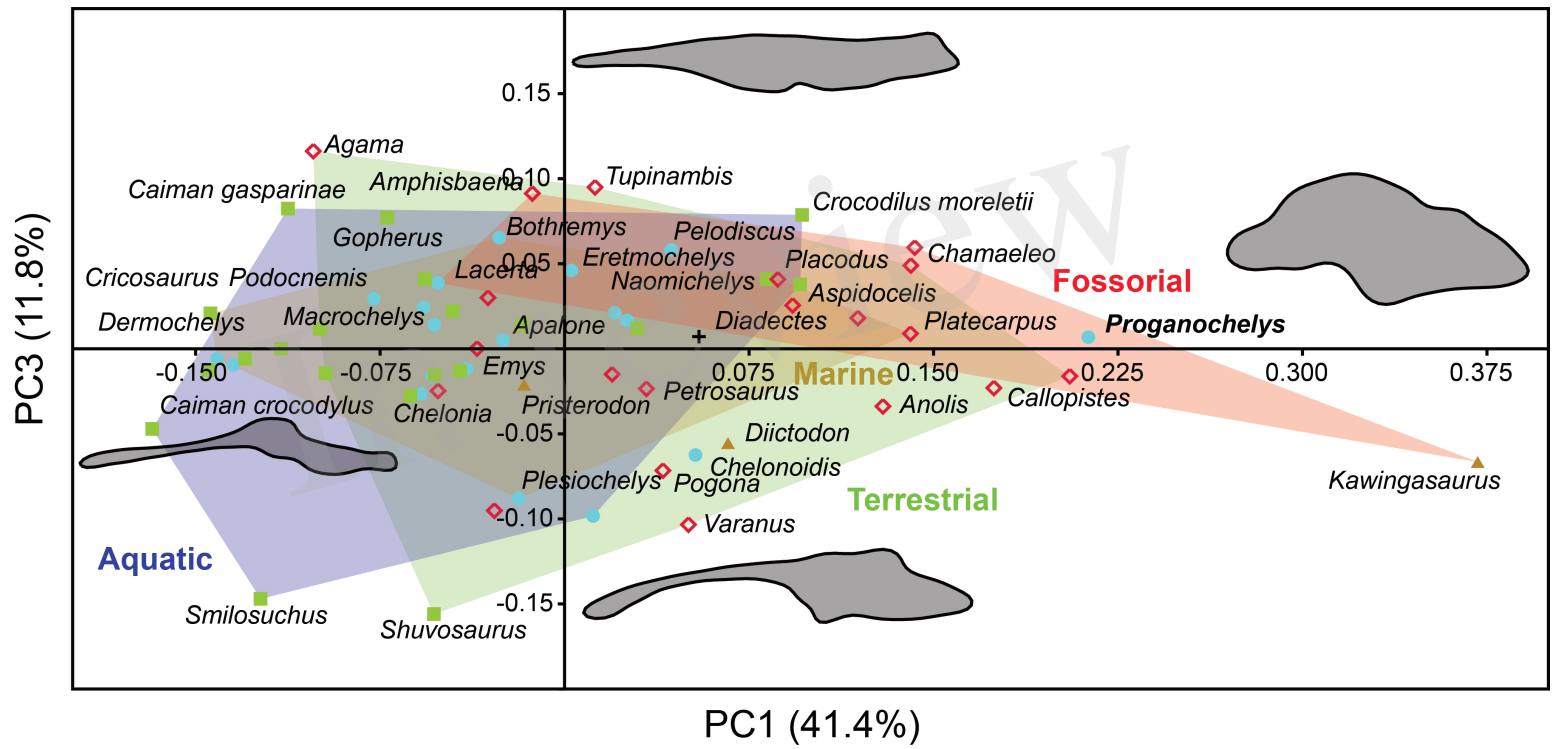
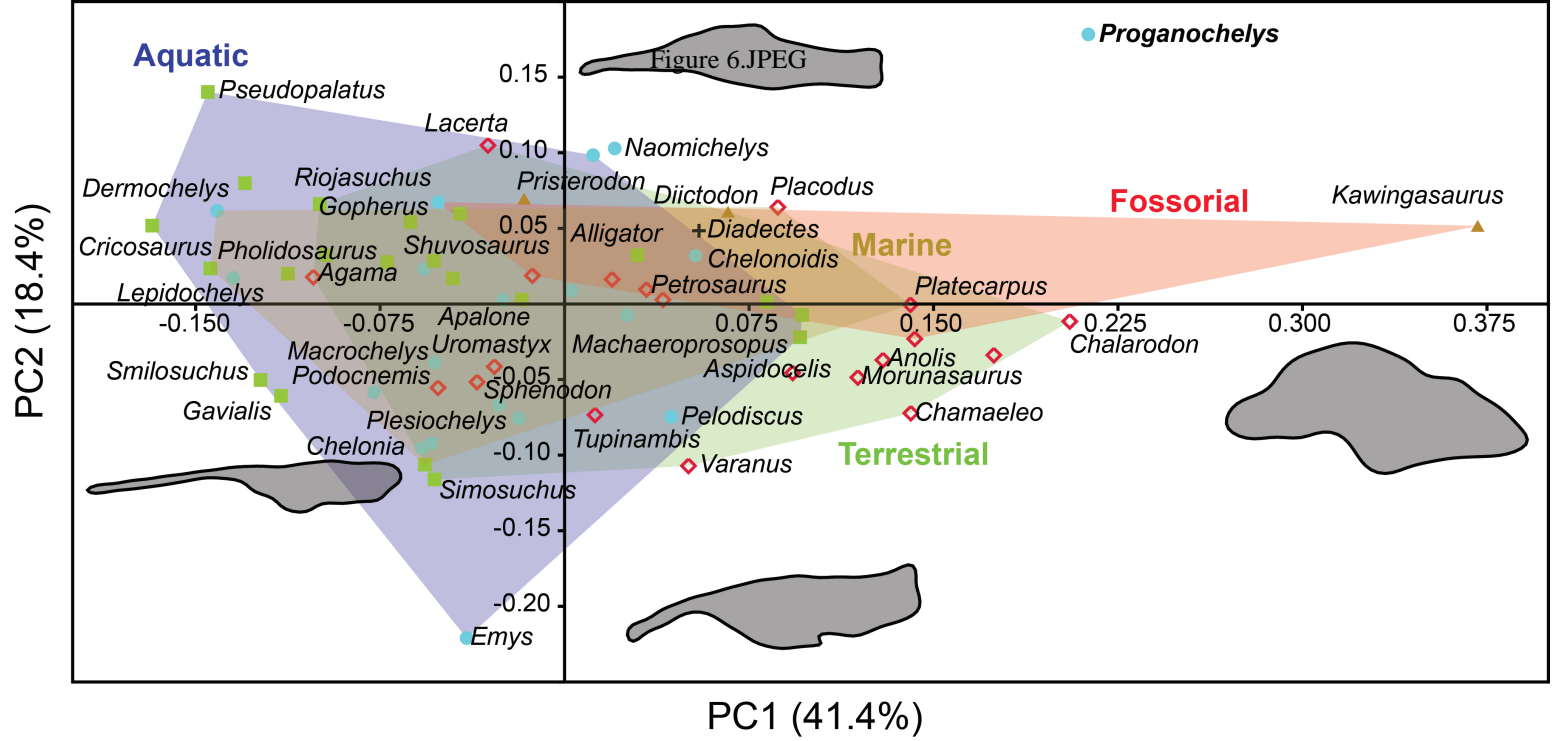


Figure 7.JPEG

